

Accepted Manuscript

Design, synthesis, structure-activity relationship and mechanism of action studies of a series of 4-chloro-1-phthalazinyl hydrazones as a potent agent against *Leishmania braziliensis*

Angel H. Romero, Rafael Medina, Anamaría Alcalá, Yael García-Marchan, Jorge Núñez-Duran, Jacques Leañez, Ali Mijoba, Carlos Ciangherotti, Xenón Serrano-Martín, Simón E. López

PII: S0223-5234(17)30030-2

DOI: [10.1016/j.ejmech.2017.01.022](https://doi.org/10.1016/j.ejmech.2017.01.022)

Reference: EJMECH 9173

To appear in: *European Journal of Medicinal Chemistry*

Received Date: 11 October 2016

Revised Date: 12 January 2017

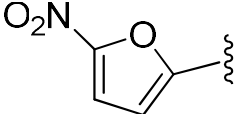
Accepted Date: 13 January 2017

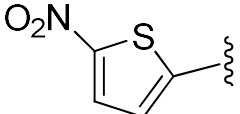
Please cite this article as: A.H. Romero, R. Medina, A. Alcalá, Y. García-Marchan, J. Núñez-Duran, J. Leañez, A. Mijoba, C. Ciangherotti, X. Serrano-Martín, S.E. López, Design, synthesis, structure-activity relationship and mechanism of action studies of a series of 4-chloro-1-phthalazinyl hydrazones as a potent agent against *Leishmania braziliensis*, *European Journal of Medicinal Chemistry* (2017), doi: 10.1016/j.ejmech.2017.01.022.

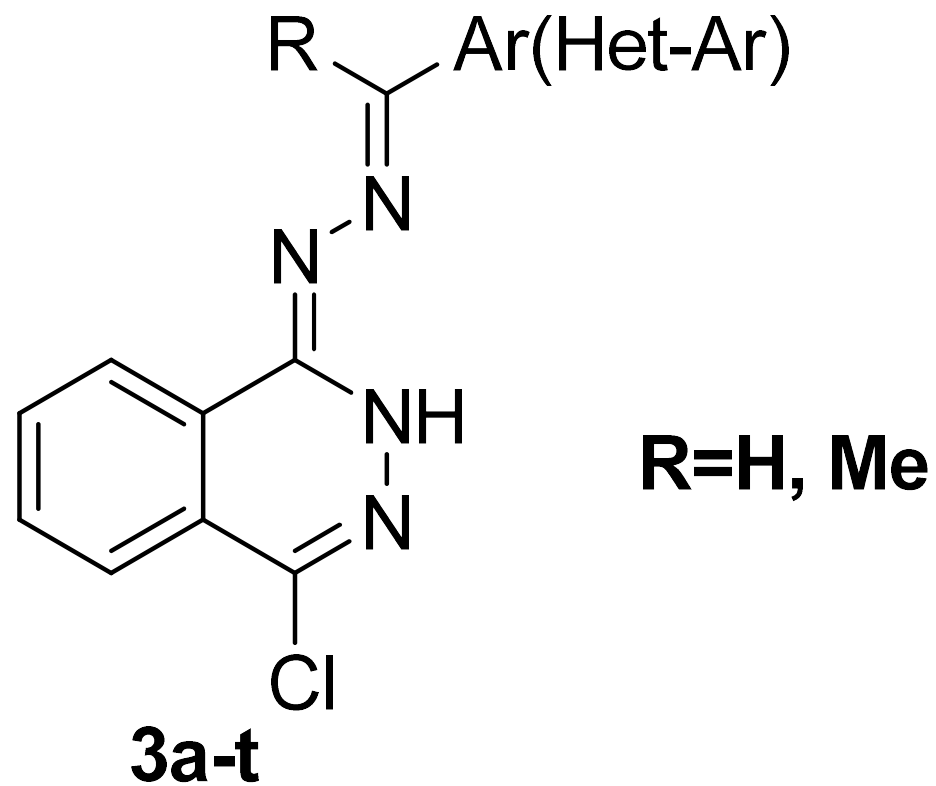
This is a PDF file of an unedited manuscript that has been accepted for publication. As a service to our customers we are providing this early version of the manuscript. The manuscript will undergo copyediting, typesetting, and review of the resulting proof before it is published in its final form. Please note that during the production process errors may be discovered which could affect the content, and all legal disclaimers that apply to the journal pertain.



<u>R</u>	<u>Ar(Het-Ar)</u>	Promastigote <u>EC₅₀ (μM)</u>	Amastigote <u>EC₅₀ (μM)</u>
----------	-------------------	---	---

H		0.12	0.59
---	---	------	------

H		3.20	
---	---	------	--



Design, Synthesis, Structure-Activity Relationship and Mechanism of Action Studies of a Series of 4-chloro-1-phthalazinyl hydrazones as a potent agent against *Leishmania braziliensis*

Angel H. Romero^{a*}, Rafael Medina^b, Anamaría Alcalá^c, Yael García-Marchan^c, Jorge Núñez-Duran^c, Jacques Leañez^c, Ali Mijoba^c, Carlos Ciangherotti^d, Xenón Serrano-Martín^c and Simón E. López^{a*}

^aLaboratorio de Química Medicinal y Heterociclos, Departamento de Química, Universidad Simón Bolívar, Valle de Sartenejas, Baruta, Caracas 1080-A, Apartado 89000, Venezuela.

^bLaboratorio de Bioquímica, Estructura y Función de Proteínas, Área de Salud, Instituto de Estudios Avanzados (IDEA), Caracas, Venezuela.

^cLaboratorio de Biología y Quimioterapia de Parasitosis Tropicales, Área de Salud, Instituto de Estudios Avanzados (IDEA), Caracas, Venezuela.

^dLaboratorio de Neuropeptidos, Unidad de Farmacología, Facultad de Farmacia, Universidad Central de Venezuela, Apartado 47206, Los Chaguaramos, 1041-A, Caracas, Venezuela.

***Corresponding authors.** E-mail:angel.romero12@ucv.ve; slopez@usb.ve

Phone: +582126052699

ABSTRACT

With the aim to identify a potential drug candidate to treat cutaneous leishmaniasis, a series of 1-phthalazinyl hydrazones were synthesized and tested against *Leishmania braziliensis* parasite, one of the main responsible of this disease in the world. A structure-activity relationship permitted to identify two phthalazines containing nitroheterocyclic moiety **3l** and **3m** as promising new lead compounds. These compounds showed a significant antileishmanial activity against promastigote form of *L.braziliensis*, with EC₅₀ values in sub-

micromolar and nanomolar ranges. The phthalazine **31** also displayed a selective and excellent activity against the clinically relevant intracellular amastigotes form, with a EC_{50} value in sub-micromolar range ($0.59 \mu M$), without affecting the viability of the host cells. Oxidative stress was identified as the possible mode of action of the most active phthalazine. Considering their significant antileishmanial activity and ease synthesis, the phthalazine containing nitroheterocyclic represents a promising agent against *Leishmania braziliensis* for the rational design of new leads.

Keywords: *Leishmania braziliensis*, antileishmanial activity, superoxide dismutase, promastigotes, phthalazine, nitroheterocycle.

1. Introduction

Leishmaniasis is a neglected tropical disease caused by at least twenty different species of the genus *Leishmania* protozoan that are transmitted to humans by the bite of infected female phlebotomine sandflies [1-5]. There are three main forms of the disease: visceral leishmaniasis (VL); mucocutaneous leishmaniasis (MCL) and cutaneous leishmaniasis (CL), being the last one the most common form of the disease [5]. More than 550 million people are at risk of infection with *Leishmania* ssp. in at least 102 countries worldwide, with an annual incidence of more than 14 million people infected, leading to 50,000 deaths [6]. According to World Health Organization (WHO), the majority of cases and deaths caused by Leishmaniasis are associated to visceral and cutaneous leishmaniasis, registering between 0.2 and 0.4 million cases of visceral leishmaniasis, and from 0.7 to 1.2 million cases of cutaneous leishmaniasis each year [7]. In particular, *Leishmania braziliensis* is the responsible of nearly 90% of all CL cases registered annually in South America, and absence or incomplete treatment promotes the subsequent development of muco-cutaneous leishmaniasis, causing permanent lesions in the mouth, nose or genital mucosa [8]. In recent decades, the number of

cases of Leishmaniasis is increasing globally due to Leishmania/HIV co-infection [9], international travels and migration [10,11]. Currently, pentavalent antimonials such as Pentostam (sodium stibogluconate) and glucantime (*N*-methylglucamine antimonate) are the first line of antileishmanial drug in many areas [12]. Nevertheless, the therapy is expensive, requiring repeated parenteral administration, higher dosages cause severe toxic side effect and in many cases have resulted to be ineffective [13]. Furthermore, large-scale clinical resistance to pentavalent antimonials has been registered in endemic areas [12a, 14]. As a consequence to the several disadvantages of pentavalent antimonials, a second line drugs including amphotericin B and miltefosine (Figure 1) has emerged as an alternative for treating of visceral and cutaneous leishmaniasis [12a, 15], although their use also has been limited because of its high toxicity and effectiveness against different forms of *Leishmania*, including *Leishmania braziliensis*.

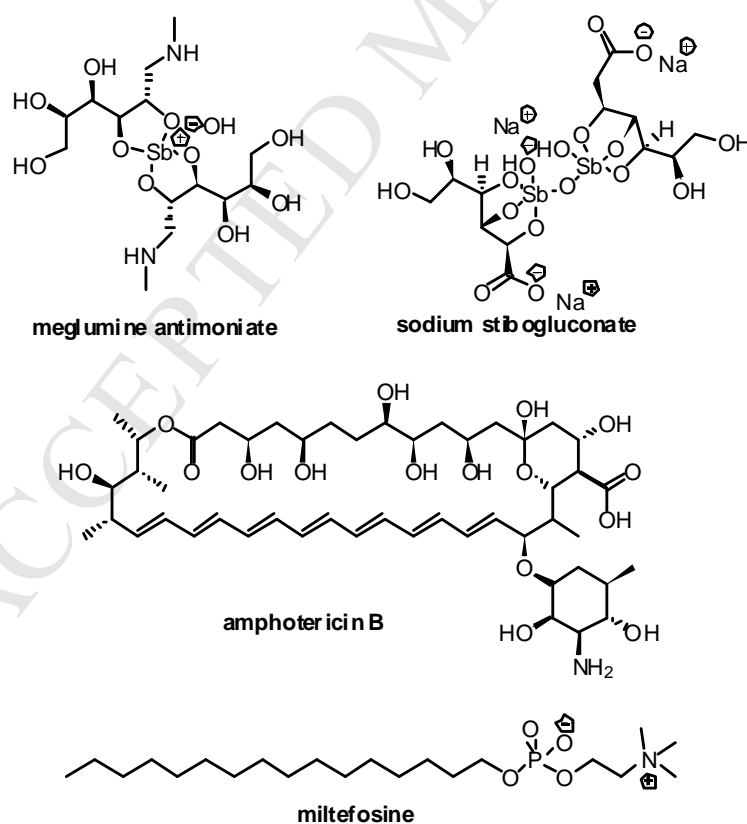


Figure 1. Drugs used to treatment of Leishmaniasis.

Then, considering toxicity issues, increasing failure rates of current treatments, increasing parasite resistance and the lack of effective clinical agents against cutaneous leishmaniasis, there is a great and urgent need the development of effective and safe new drugs for treating of leishmaniasis in their different clinical forms. In this sense, an enormous variety of potent and active new heterocycles have emerged during the last decade against different *leishmania* spp., including quinolines [16-17], quinazolines [18-23] and phthalazines [24].

2. Results and discussion

2.1. Design and synthesis of the target compounds

To design new potential drugs, it is important to understand the essential metabolic biochemical pathways or crucial parasite-specific enzyme. Trypanothione reductase, cysteine protease, dihydrofolate reductase, glyceraldehyde 3-phosphate dehydrogenase, superoxide dismutase (Fe-SOD) and oxidative stress have emerged as interesting targets [25]. In this investigation, we focused our attention on iron superoxide dismutase (Fe-SOD) and oxidative stress for the design of our new antileishmanial compounds. Fe-SOD enzyme plays an important role in the defence of trypanosomatids against oxidative agents and it is not present in humans. Some evidences in trypanosomatids have shown that parasitic protozoan survival is closely related to the ability of that enzyme to suppress toxic free radical damage originated by their host [26]. The enzymatic activity of Fe-SOD is directly associated to the iron metal contained into active site of the enzyme and it represents an attractive target for the development of new agents based in complexation with iron metal. In recent years, Sanchez-Moreno's group has designed new phthalazines and benzo[g]phthalazines functionalized in positions 1 and 4 of the pyridazine ring with flexible alkylamine side chains, which have shown a significant inhibition of the SOD enzyme of *T.cruzi*, *L.infantum* and *L.braziliensis* parasites. The inhibitory activity of these compounds showed a direct correlation with their

respective anti-trypanosomatids activity against *L.infantum*, *L.braziliensis* and *T.cruzi* [24, 27].

On the other hand, the induction of oxidative stress by using of nitroheterocyclic compounds has been little explored against *Leishmania* parasites. This target is more common in the design of antichagasic agents and it generates unstable highly toxic reduced oxygen species from redox-cycling metabolism that damages proteins, lipids and DNA, leading to parasite death [28-29]. Many oxidative stress inductors are based in a nitro-heterocyclic segment [29]. Thus, it results very interesting to develop an antileishmanicidal agent that acts by both mechanism because the inactivation of SOD enzyme could reduce significantly the defences of parasite against the toxic radical species generated by the possible bio-reduction of the nitro-compound. On these bases, we consider in our design a nucleus of phthalazine, related to the SOD inhibition, connected to a segment of aryl or heteroarylhydrazone, crucially important in the induction of oxidative stress when the aryl/heteroaryl moiety is represented by a nitrofuryl or nitro-thiophene group. Interestingly, crystal structures of mononuclear complexes with transition metals such as mercury (II), molybdenum (V) and others [30] have been found for some 1-phthalazinyl-arylhydrazones. Therefore, it is possible to think that the designed phthalazines **3a-t** may form a complex with the iron (II) metal, being a potential Fe-SOD inhibitor in *Leishmania* parasites (**Figure 2**).

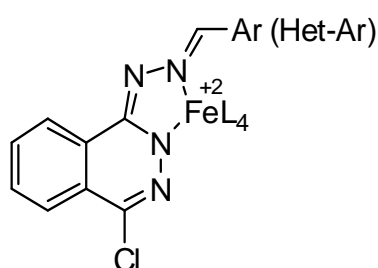
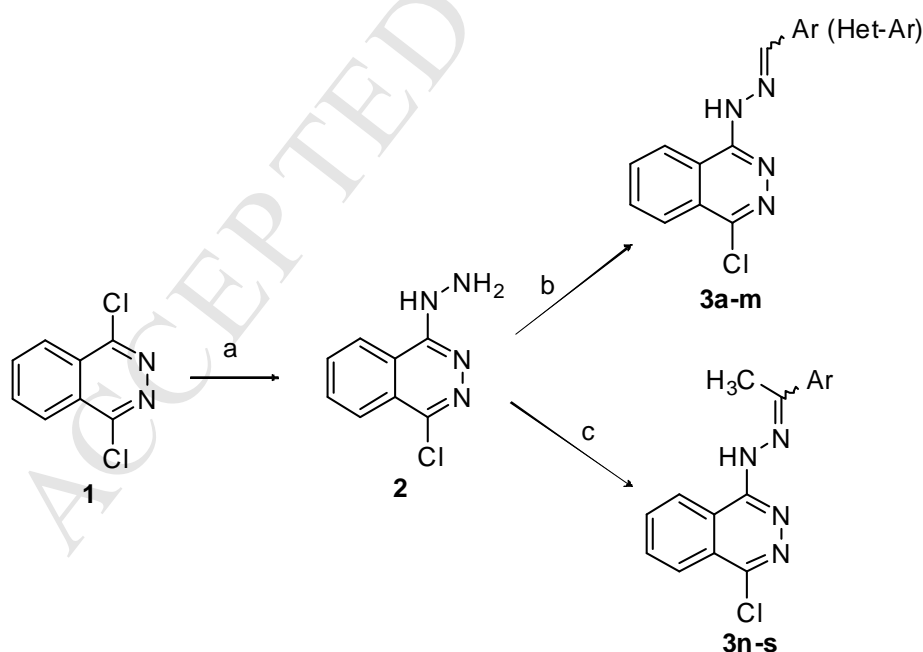


Figure 2. Possible complex between Fe and 4-chloro-1-phthalazinyl hydrazones.

2.2. Synthesis section

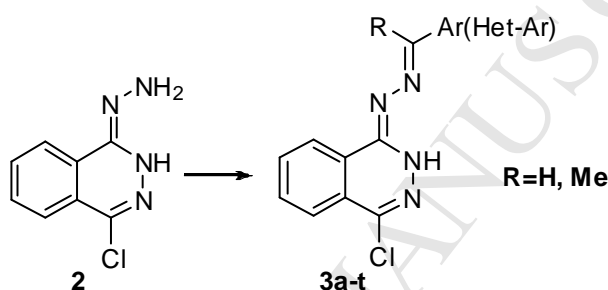
The preparation of title phthalazines **3a-t** involved a two-step facile procedure from commercially available starting materials according to experimental protocols reported in the literature, with a few modifications [31]. The general synthesis of the phthalazinyl-hydrazones **3a-t** is depicted in **Scheme 1**. Thus, step 1 involves a S_NAr reaction between 1,4-dichlorophthalazine **1** and hydrazine monohydrate under reflux to provide the desired 1-chloro-4-hydrazinylphthalazine **2** in good yield (83 %). Next, the sequence involves an acid catalyzed condensation of compound **2** with the corresponding aromatic aldehyde or acetophenone to give their respective substituted phthalazines **3a-m** and **3n-t**. This last reaction displayed excellent yields, ranging from 85 to 97 %, with exception of derivatives **3s** and **3t** (see **Table 1**). In particular, this reaction required extended times when acetophenones were used. The experimental details and the spectroscopic data for the intermediary **2** and phthalazine derivatives **3a-t** are shown in the supporting information.



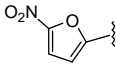
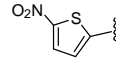
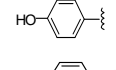
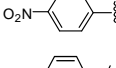
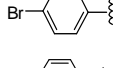
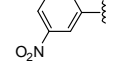
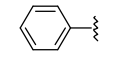
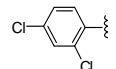
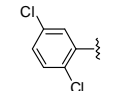
Scheme 1. Synthesis of phthalazin-hydrazone derivatives **3a-t**. Conditions: (a) N₂H₄.xH₂O, Ethanol, reflux, 2 h; (b) Aryl/heteroaldehyde, HCl (1M), 60°C, 10 min.; (c) Acetophenone, HCl (1M), 60 °C, 2-10 h.

In general, based in the chemical shift found for the ylidene proton of the compounds **3a-t** in the ^1H NMR spectra and that information reported for some of their derivatives and analogues, it is possible to conclude that most of the prepared phthalazinyl-hydrazones present a *E*-configuration around the imine (H-C=N) double bond, with exception of the derivative **3i** that has a *Z*-configuration [32]. A detailed analysis concerning to the assignment of *E* or *Z* configuration for the synthesized compounds is shown in the supplementary material.

Table 1. Yields in the last step for the synthesis of the phthalazine derivatives **3a-t**.



Compd No.	Ar (Het-Ar)	R	Yield (%)	m.p. (°C)	Diastereoselection ^a
3a		H	96	173-174 (Lit. 175-176) ^b	<i>E</i>
3b		H	92	184-186	<i>E</i>
3c		H	94	255-257	<i>E/Z</i> (94/6)
3d		H	91	220-222	<i>E/Z</i> (96/4)
3e		H	88	203-205	<i>E/Z</i> (93/7)
3f		H	90	235-238	<i>E</i>
3g		H	87	217-218	<i>E</i>
3h		H	88	196-198	<i>E</i>
3i		H	87	157-160 (Lit. 162-163) ^b	<i>Z</i>
3j		H	91	246-248	<i>E</i>
3k		H	89	170-172	<i>E</i>

3l		H	93	230-232	<i>E/Z</i> (93/7)
3m		H	85	220-222	<i>E/Z</i> (93/7)
3n		CH ₃	97	212-214	<i>E</i>
3o		CH ₃	79	234-236	<i>E</i>
3p		CH ₃	88	182-184	<i>E</i>
3q		CH ₃	93	217-219	<i>E</i>
3r		CH ₃	73	142-144	<i>E</i>
3s		CH ₃	50	162-164	<i>E</i>
3t		CH ₃	42	166-168	<i>E</i>

^aGeometric configuration and mixture of diastereomers for each phthalazine **3a-t** was predicted by a detailed comparative analysis between the chemical shift of ylidene proton found in their corresponding ¹H NMR spectra and the information available in literature [32].^b Melting points are taken from ref. [31a] for these reported compounds.

2.3. Biological evaluations

2.3.1. *In vitro* antileishmanial activity and structure-activity relationships

The aim of this study was to determine the importance of phthalazinyl and aryl/heteroarylhydrazone moieties as potential pharmacophores in the design of our new antileishmanial agents. To reach this goal, twenty phthalazines **3a-t** coupled to different aromatic systems (i.e., substituted arylidenes and heteroarylidenes) were initially tested *in vitro* against *L. braziliensis* parasite, evaluating its effect on promastigotes growth to a specific concentration of 20 μ M for each compound. In this first screening, the derivatives **3c**, **3l** and **3m** showed the most significant ability to inhibit the promastigote proliferation of *L. braziliensis*, with PGI values of 58.14 %, 86.49 % and 88.46 %, respectively (see **Table 2**). A weak antileishmanial activity was observed for the rest of compounds with low PGI values

(<40) at 20 μM ($\text{EC}_{50}>20 \mu\text{M}$) (**Table 2**), which demonstrates the important role of the nitro-substitution in the antileishmanial activity of the tested compounds. After the first screening, the concentration response data for the most active derivatives **3l** and **3m** was fitted by a nonlinear regression model, and the concentration that induces 50% inhibition was calculated as the effective concentration EC_{50} on *L.braziliensis* promastigotes. These derivatives **3l** and **3m** affected the viability of *L. braziliensis* promastigotes, with EC_{50} values of 0.12 and 3.20 μM , respectively (**Table 3**). Both derivatives **3l** and **3m** were more potent than miltefosine against promastigotes of *L.braziliensis* by a factor of 208 and 8, respectively. This result is interesting due to that miltefosine is the first oral drug used for visceral leishmaniasis treatment and it has been considered a major breakthrough in antileishmanial chemotherapy [33].

Table 2. Preliminary evaluation on the *L.braziliensis* promastigotes growth, theoretical ZDO atomic charges on the ylidene carbon and absorption maxima (λ_{max}) for the tested phthalazinyl-hydrazones **3a-t**.

Entries	Compound	PGI (%) ^{a,b}	EC_{50} (μM) ^b	$\text{ZDO}_{\text{C=N}}$ ^c	λ_{max} ^d (nm)
1	3a	8.46	>20	-0.0449	372
2	3b	17.78	>20	-0.0505	369
3	3c	58.14	<20	-0.0863	420
4	3d	17.21	>20	-0.0546	372
5	3e	16.75	>20	-0.0516	368
6	3f	10.58	>20	-0.0791	391
7	3g	5.89	>20	-0.0563	367
8	3h	7.03	>20	-0.0572	368
9	3i	33.85	>20	0.0300	364
10	3j	11.86	>20	-0.0651	389
11	3k	40.86	≥ 20	-0.0441	376
12	3l	86.49	0.12	-0.0924	475
13	3m	88.46	3.20	-0.0849	496

14	3n	22.91	>20	-0.0248	372
15	3o	19.08	>20	-0.0651	430
16	3p	10.62	>20	-0.0404	374
17	3q	9.46	>20	-0.0554	390
18	3r	36.95	>20	-0.0329	374
19	3s	37.47	>20	-0.0466	375
20	3t	19.98	>20	-0.0497	376
21	Miltefosine ^e	67.78	<20	N.D	N.D
22	Control (-) ^f	0.02	-----	-----	-----

^aProliferation growth inhibition (PGI), doses=20 μ M. ^bThe results are the means of three independent experiments with a SD less than 6% in all cases. ^cZDO charge on ylidene carbon. ^d λ_{max} was measured in methanol as solvent. ^eMiltefosine was used as reference drug. ^fUntreated control. N.D.: not determined.

A detailed analysis of the structure-activity relationship for the evaluated phthalazines **3a-t** permitted us to establish the following remarks:

- The substitution of a specific arylidene group by a nitroheteroarylidene group linked to hydrazone scaffold increases significantly the antileishmanial activity of the synthesized phthalazine (compare **3l** and **3m** with the rest of compounds).
- The substitution of oxygen by sulphur in the heterocyclic ring reduces almost 27 times the antileishmanial activity, reflecting the importance of the furyl group in the mentioned biological activity over thiophene ring in our phthalazin-derivatives.
- The nitro-substitution at the *para*-position of arylidene system increases the antileishmanial activity with respect to their arylidene phthalazin-analogues.
- Replacement of the hydrogen atom (**3a-m**) by the methyl group (**3n-t**) around the imine double bond (C=N) of synthesized phthalazines decreases the antileishmanial activity in most of the analogues cases (compare **3a**, **3c**, **3d**, **3f** vs. **3r**, **3o**, **3p**, **3q**, Table 2).
- Localization of the nitro group at the *orto*-position or *meta*-position of arylidene system (**3f**, **3j** and **3q**) represents a significant loss of biological activity.

- f) The introduction of halogens (F, Cl, Br) (**3d-f**, **3g-h**, **3p-t**) and electron-donating groups (**3j**, **3n**) in the arylidene system makes phthalazines less active.

These evidences suggest that the antileishmanial activity of the studied phthalazine-hydrazones is associated to the highly conjugated aryl/heteroaryl hydrazone scaffold due to that only the nitro-derivates **3c**, **3l** and **3m** exhibited the most significant biological response. The specific localization of the nitro group at the position “4” and “5” of aryl and heteroaryl moieties of phthalazine derivative, respectively, facilitates an optimal π -electron conjugation from hydrazinyl group to nitro group. Thus, in order to understand this correlation between high conjugation and biological activity, we decide to calculate the ZDO atomic charges on the ylidene carbon of all phthalazines due to that this carbon atom is an important bridge for the π -electron delocalization from hydrazinyl group to aryl or heteroaryl group. A high negative character on the ylidene carbon indicates that there is a significant π -electron conjugation between the mentioned segments, which can be to facilitate by a strong electron-deficient heteroaryl or aryl moieties. The theoretical values of ZDO atomic charges were performed using the semi-empirical method AM1 for the optimized geometry of all investigated derivatives and the results are shown in Table 2. From data, it is clear to appreciate a direct relationship between the electronic nature of the ylidene carbon and the antileishmanial activity, where the most active compounds (**3c**, **3l** and **3m**) presented the most negative ZDO atomic charge on the above mentioned carbon, which confirms the important role of an nitro-heteroaryl highly conjugated in the antileishmanial activity of our phthalazine compounds. This theoretical evidence permits to explain the higher potency found for the compound **3l** (major ZDO) in comparison with the compounds **3c** and **3m**. The high conjugated nature of the active nitro-derivatives (**3c**, **3l** and **3m**) was experimentally confirmed by their highest λ_{\max} values from 420 to 496 nm (see Table 2). Thus, the significant importance of the π -electron delocalization of the nitro-derivative in the antileishmanial activity suggests that the most

active derivatives can be involved in an electron transfer reaction of the redox metabolism of the parasite, which is facilitated by the partial stabilization of the radical intermediaries formed that provides this high π -electron delocalization in the phthalazine system. This type of mechanism has been widely reported for antichagasic nitro-drugs such as nifurtimox and benznidazole on *T. cruzi* [34] and more recently on *L. donovani* [29]. In the mechanism of action section is shown a preliminary study that demonstrates the potential of **3l** as inductor of oxidative stress.

On the other hand, the poor antileishmanial activity found for the rest of synthesized nitro-derivatives such as **3f**, **3j**, **3o** and **3q** can be explained by their moderate negative ZDO charge, by comparison with **3c**, **3l** and **3m** (see Table 2).

The relative major importance of the ylidene hydrogen (H-C=N) with respect to the methyl moiety (CH₃-C=N) seems to be associated to the higher negative charge character on the ylidene carbon of the phthalazines **3a-m** (R=H) than on the carbon of their analogues **3n-t** (R=Me) (compare ZDO of the entries 3 and 15 of Table 2).

As we expected, compounds with the lower negative ZDO charge on the ylidene carbon showed the lowest antileishmanicidal activity. Among these derivatives, it can be mentioned those functionalized with electron donating groups (**3i** and **3n**), halogens (**3b**, **3d-e**, **3g-h**, **3p** and **3s-t**), unsubstituted (**3a** and **3r**) and *meta*-nitro group (**3f** and **3o**). However, derivatives **3i** and **3k** particularly exhibited a moderate inhibition on promastigote growth, with PGI values of 33.85 and 40.86, respectively. This last suggest that the moderate antileishmanial of these two compounds can be associated to a non-electron dependent mechanism, such as a *Leishmania* SOD inhibition. This hypothesis was considered and examined theoretically by a docking computational study on SOD enzyme, where **3i** and **3k** exhibited a better interaction into SOD binding site than the compounds **3c**, **3l** and **3m** (see table 6, molecular docking

studies section). This result should not be surprising due to that these phthalazines represent a potential tridentate ligand which can form a stable complex with different metals [30].

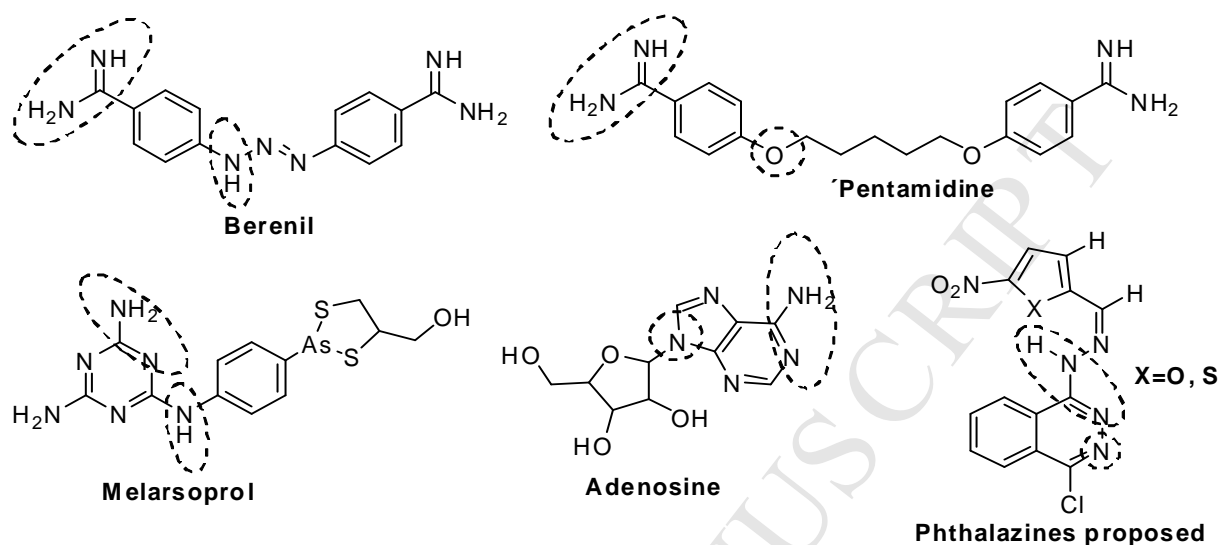


Figure 3. Substrates of the P2 transporter. Remarked circles indicate the group involved in the interaction with the membrane [37].

Finally, in order to know the importance of the phthalazine nucleus in our derivatives, the antileishmanial activity was analyzed for a series of analogues containing a nitrofurylaryl-hydrazinyl scaffold linked to a nucleus of phthalazine (our compounds), quinoline [35], melanine [36] and aliphatic unit (nifurtimox) [29,36]. The comparative analysis demonstrates that the electron-deficient nature of these conjugated nucleus (phthalazine, quinoline and melanine) play an important role in antileishmanial activity due to the significant antileishmanial response found in their respective compounds. While a no-conjugated nucleus (a saturated aliphatic unit) connected to the nitroheterocyclic moiety such as in nifurtimox displayed a moderate antileishmanial activity. This last suggest that the presence of the phthalazine (or quinoline, melanine) generates a system highly conjugated from phthalazin ring to the nitro group of heteroarylidene moiety, which seems to be crucial in the antileishmanial activity. Although it is important to mention that probably the phthalazine nucleus is not responsible of the biological response because in most of the tested compounds

was observed a poor antileishmanial activity. In addition, due to the structural similarity between the phthalazin-hydrazinyl scaffold and the amidine moiety (see Figure 3), an important substrate of P2 that is present in the cell membrane of the trypanosomatids and facilitate the accumulation of the compound into pathogen [37], the phthalazine nucleus can play an important role in the transportation of the agent within the parasite.

2.3.2. Cytotoxicity assays

The cytotoxicity of compounds **3l**, **3m** and miltefosine was evaluated using macrophages of a BMDM cell line derived from narrow mouse [38], and the results are listed in Table 3. In particular, derivative **3l** showed a moderate *in vitro* toxicity with a LD₅₀ value of 14 μ M, however that compound displayed an excellent selectivity index (SI) value of 116.7 (see Table 3), being much more destructive to the parasitic form than the host cells. Additionally, the selective index confirms the apparent advantage found *in vitro* for the compound **3l** with respect to reference drug miltefosine. Contrary to **3l**, compound **3m** resulted to be highly toxic on this host at low concentration (LC₅₀<10 μ M). Then, in this case, the nitro-thiophene moiety can be responsible of the significant toxicity found for the compound **3m**. The moderate and high toxicity found for the two active derivatives on macrophages and the known mutagenic effect caused by the nitro-derivatives on mammalian cells [39], suggests that genotoxicity assays are necessary for future investigations.

Table 3. Effect of phthalazines **3l**, **3m** and miltefosine on BMDM macrophages and EC₅₀ values (μ M) on *L.braziliensis* promastigotes.

	Macrophages BMDM LC ₅₀ (μ M) ^a	Promastigotes EC ₅₀ (μ M) ^a	Selectivity index
3l	14.00 \pm 0.25	0.12 \pm 0.01	116.7
3m	<10.00	3.20 \pm 0.92	<3.0
Miltefosine^b	125.00 \pm 4.70	25.00 \pm 1.40	5.0

^aThe results are the means of three independent experiments with a SD less than 6% in all cases. ^b Miltefosine was used as reference drug.

2.3.3. Intracellular amastigote evaluation

Going one step further in the activity study, leishmanicidal effect of phthalazine **31** on amastigote stage was carried out through an *in vitro* infection model consisting of macrophages BMDM infected by *L. braziliensis* amastigote. Using this model, a 40% maximum infection was obtained, similar to previous studies [40]. The effect of **31** was evaluated at 96 hours post-treatment and the results were shown graphically in the Figure 4. It should be noted that phthalazine **31** also is significantly active against amastigote stage of *Leishmania braziliensis*, evidenced by the monotonic decrease in the number of amastigotes and infected macrophages to the tested concentrations, leading to a EC₅₀ value of 0.59 μM for the compound **31**. It is important to emphasize that this effect is highly selective against intracellular amastigotes without affecting the viability of host cells (BMDM macrophages). This anti-amastigote response found for the compound **31** is extremely important because this stage is the main responsible of the clinical manifestations of leishmaniasis. Furthermore, the significant selectivity found for **31** on promastigotes and amastigotes with respect to the macrophages cells, as well as its excellent potency, permits to consider to **31** as a promising antileishmanial lead. Table 4 shows the selectivity indexes of **31** on the promastigotes and amastigotes stages of *L. braziliensis*, as well as their specificity.

Table 4. Effect of phthalazine **31** on BMDM macrophages, EC₅₀ values (μM) on promastigote and amastigote of *L. braziliensis*, selectivity and specificity indexes.

	Macrophages BMDM LC ₅₀ (μM)	Promastigote EC ₅₀ (μM)	Amastigote EC ₅₀ (μM)	Selectivity index ^a	Selectivity index ^b	Specificity index ^c
31	14.00 ± 0.25	0.12 ± 0.01	0.59 ± 0.13	116.7	23.7	4.9

^aSelectivity: LC₅₀ of macrophages/EC₅₀ of promastigotes of *L. braziliensis*.

^aSelectivity: LC_{50} of macrophages/ EC_{50} of amastigotes of *L. braziliensis*.

^bSpecificity: is the ratio between amastigote EC_{50} and intracellular promastigote EC_{50} .

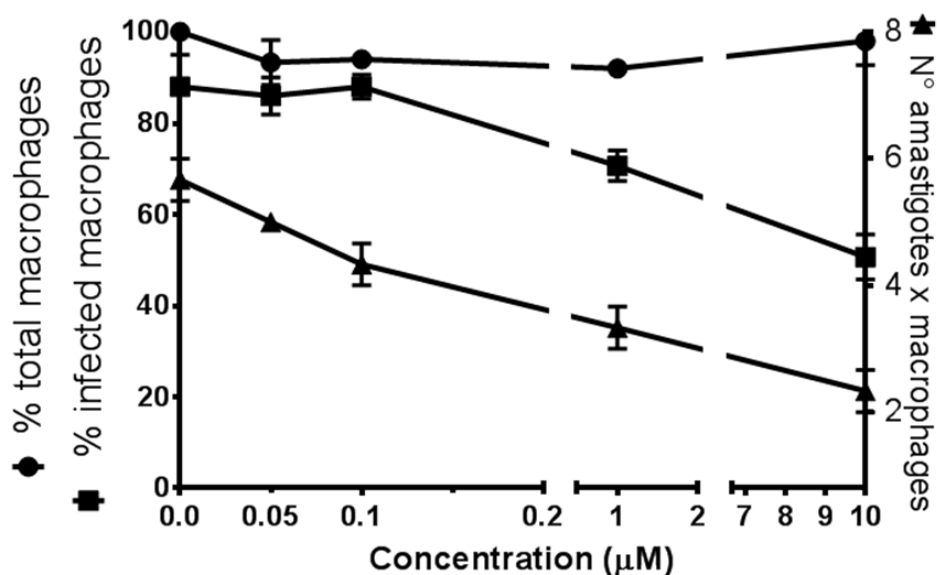


Figure 4. Evaluation of phthalazine **31** on intracellular amastigotes of *L. braziliensis*. Dose-response curve, BMDM macrophages were infected with promastigotes of *L. braziliensis* (1:10) and incubated with **31** for 96 h. % macrophages total (solid circle line), % infected macrophages (solid square line) and N° amastigotes x macrophages (solid triangle line). Each experiment was carried out by triplicate.

As last topic in this section, a detailed analysis concerning to the antileishmanial activity against amastigote found for derivatives of phthalazine (our derivative), quinoline [35] and melanine [36] linked to the nitrofurylhydrazinyl permits us to conclude that the nucleus of phthalazine and quinoline can represent an important moiety in the specificity on amastigote form due to their significant response in ranges nanomolar. In this sense, it results very interesting to explore other mechanism of action related with the system macrophage-amastigote such as the generation of nitric oxide (NO) (see section mechanism action studies).

2.4. Mechanism Action Studies

In order to validate our hypothesized mechanism of actions, the inhibition of the SOD parasite enzyme and induction of oxidative stress were evaluated preliminarily for the most active compound **31**. In addition, other two possible targets such as the generation of nitric oxide from macrophages induced by the action of the drug and the dihydrofolate reductase inhibition were explored.

The oxidative stress mechanism was evaluated by the measurement of the mitochondrial dehydrogenase activity on *L.braziliensis* promastigote in the absence and presence of the compound **31**. It is well known that oxidative stress has important effect in the mitochondrial dehydrogenase activity and its measurement at short time permits us to estimate qualitatively whether an oxidative stress mechanism is generated in the system [41a-c]. Free radical attack generated by oxidative stress occurs directly at complexes in the mitochondrial respiratory chain. Specifically, complexes I and III are also thought to be major sites for the production of superoxide and other reactive oxygen species [41d] and the high reactivity of these species can damage macromolecules within mitochondria, including lipids, proteins and DNA [41e]. Thus, this mitochondrial DNA damage affects to the complex I and/or III function, inducing to an increase in the electron reduction of O₂ to superoxide ion [41d, 41f-g]. On these bases, the percentage of mitochondrial dehydrogenase activities (Pmdh) with respect to untreated control and reference drug was assessed using the colorimetric MTT assay performed at very short times, between 30 min. and 180 min. of incubation, according to procedure described for *Leishmania* parasite [41h]. The results are illustrated in Figure 5. In particular, only the phthalazine **31** affect the mitochondrial dehydrogenase activity producing a decrease in a time-dependent manner, while the reference drug and untreated control did not show change in the mitochondrial dehydrogenase response. This evidence demonstrates the significant action of the compound **31** on the mentioned enzyme at very short time of incubation, which

suggests that the significant reduction of MTT in these times (inclusive 30 min) is induced by the generation of radical species from metabolized compound **31** and not by cell deaths, due to that practically no cell death was observed at these short times.

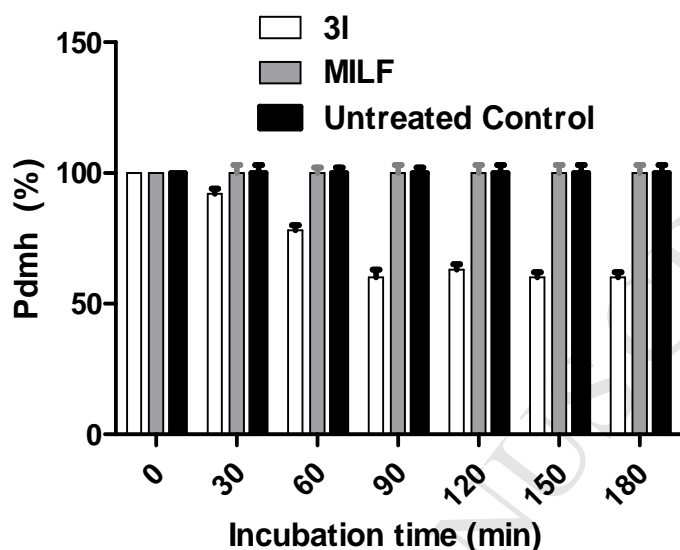


Figure 5. Variation of the percentage of mitochondrial dehydrogenase activities (Pdmh), produced by the compound **31** exposed to an incubation time, compared to untreated control and miltefosine (MILF).

In order to explore more about the oxidative stress mechanism and the significant anti-mastigote activity found for the compound **31**, we decided to study an interesting target such as the generation of nitric oxide induced by action of the phthalazine **31** and analyze its effect on the parasite stage. In particular, the mitochondrial respiratory chain is particularly sensitive to both NO^- and ONOO^- mediated damage. Protein oxidation and nitration result in altered function of many metabolic enzymes in the mitochondrial electron-transport chain, including nicotinamide adenine dinucleotide dehydrogenase, cytochrome c oxidase, and adenosine triphosphate synthase [42a]. Some investigations have identified the generation of reactive nitrogen species as nitric oxide (NO) by macrophage as a cytotoxic molecules responsible of the intracellular parasite damage [42b-c]. Based in this idea, the correlation

between the anti-amastigote effect of the compound **31** and the generation of NO by the macrophage in the infected macrophage system was studied in this section, and the data obtained are shown in Figure 6. The corresponding PGI (%) values are included in order to establish a relationship with nitric oxide production. This assay was performed using three concentrations in turn to EC₅₀ on intracellular amastigote, including 0.08, 0.80 (~EC₅₀) and 8.0 μM for the compound **31**. From Figure 6, it should be noted that the infected macrophages treated with the compound **31** showed an increase of nitric oxide in the culture compared to untreated infected macrophage control, being the effect significantly concentration-dependent. This *in vitro* evidence indicates that the compound induces the NO production in the infected macrophage, permitting to explain the significant anti-amastigote effect of the compound **31**. In addition, a direct relationship between the anti-amastigote activity and nitrite production was observed, which suggests that definitively cell amastigote death is associated to the NO production from infected macrophage. This NO generation may be induced by phthalazine metabolism into macrophage.

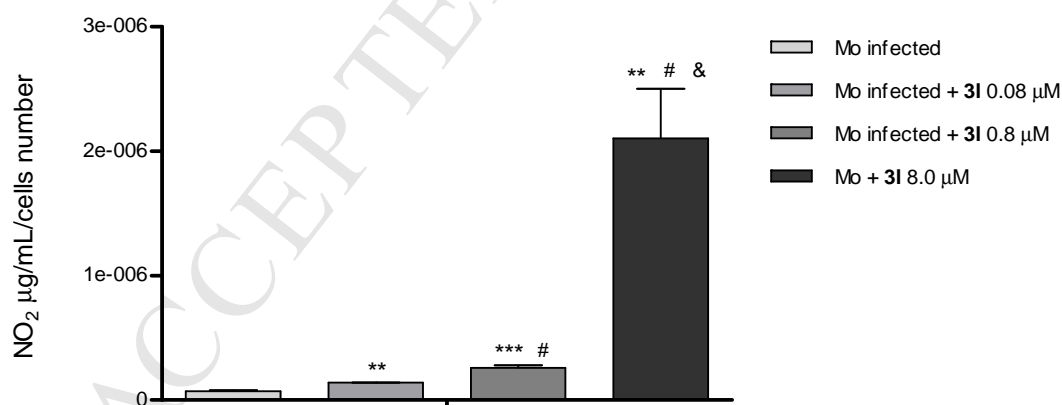


Figure 6. Effect of the compound **31** at increasing concentration from 0.8 to 8.0 μM on the production of nitrite (nitric oxide metabolite) for the system macrophages infected with *Leishmania braziliensis*. Mo, untreated macrophages infected. **p<0.01, ***p<0.001 compared to untreated macrophages infected. #p<0.01 compared to **31** 0.08 μM group. &p<0.05 compared to **31** 0.8 μM group.

In second place, the effect of **3l** was explored on the SOD activity from *L.braziliensis* promastigote as described in the literature using xantine oxidase. This assay was evaluated using three different concentrations in turn to the EC₅₀ on the promastigote stage, including 0.012, 0.12 (EC₅₀) and 1.2 μM of the compound **3l**. The results clearly revealed that no changes were observed between the parasites treated with the compound **3l** with respect to untreated control, which permits us to discard this mechanism of action, at least for the compound **3l** on *Leishmania* parasite.

In order to obtain more information about the Fe-SOD activity of the tested compounds and confirm the experimental results, a tentative molecular modelling study on their mode of interaction with the enzyme was performed. In this sense, the closest enzyme available of SOD in trypanosomatids is the SOD of *T.cruzi* (PDB ID code: 2GCP), which was taken from the Protein Data Bank and the molecular docking was evaluated for the most active derivatives **3c**, **3l** and **3m**, and the potential SOD inhibitors **3i** and **3k**. In the molecular docking study, the affinity of the most active derivatives **3l** and **3m** toward SOD enzyme was readily poor due to their lower values of docking energy into binding site (6.06 and 7.67, respectively) (see Figure 7), while the phthalazine **3i** and **3k** showed a more significant affinity with the SOD enzyme than the mentioned nitro-derivatives with values of free energy affinity of 8.90 and 9.73, respectively. These results are completely expected due to that the electron-deficient character of the nitro-substitution can affect the complexation capacity of these nitro-derivatives with iron metals. Furthermore, the presence of the hydroxyl and furyl moieties in the structure of **3i** and **3k**, respectively, reinforce the potential complexing ability of these derivatives as a tridentate ligand. This fact permits us to correlate the moderate biological activity found for the compounds **3i** and **3k** with the inhibition of the SOD enzyme. On the other hand, the moderate or poor interaction ligand-SOD into active site for our phthalazines can be explained by the localization of the phthalazines outside binding site

cavity of the SOD enzyme, which affects therefore the interaction phthalazine-iron metal (see Figure 7). In order to complement the molecular modelling, the distance between the most active compounds **3l** and **3m** and iron metal into binding site was calculated. It showed that the nitrogen atom N3 of **3l** and **3m** (nitrogen bonded to C4 of phthalazine nucleus) was located further away by about 8.21 and 7.90 Å, respectively. In addition, the phthalazines **3i** and **3k** also showed similar distances Fe-ligand by about 7.32 and 8.69 Å. The compound **3c** did not exhibit poses in the binding site of SOD enzyme. The localization of the tested phthalazines outside SOD binding site seems to be associated to that the cavity of binding site is very small with respect to the molecular size of the tested phthalazines. It is very important to explain that the high sp^2 character of the side chains in the studied phthalazines affect its molecular flexibility, which may thus affects the localization of the ligand (**3l** or **3m**) inside the active site. In this sense, in the previous experimental and theoretical studies reported for the benzo[g]phthalazines and phthalazines analogues [27] was found that the monosubstituted derivatives (minor molecular size) exhibited a better *in vitro* inhibition of the SOD enzyme than the disubstituted compounds, which was completely correlated to its significant free energy affinity ligand-enzyme and proximity ligand-iron metal in the molecular docking. These theoretical evidences permit us to conclude that some molecular factors such as the molecular size and molecular flexibility play an important role in the interaction ligand-enzyme into binding site of the SOD enzyme. In this sense, the high electron-deficient of the phthalazine-hydrazone **3l** (associated to the nitro group) and its little molecular flexibility may help to explain the no *in vitro* SOD inhibitory activity found for the compound **3l**. Finally, Table 5 shows the main H-bond and hydrophobic interactions of the compounds **3c**, **3i**, **3k**, **3l** and **3m** into binding site of the SOD enzyme.

Table 5. Docking Statistics of the compounds with TR and SOD, and their data of PGI.

Molecules ^a	SOD			PGI (%) ^c
	E_{SOD} ^b	H-bond	Hydrophobic Interactions	
3c ^d	N.F.	N.F.	N.F.	41.86
3i	-8.90	31His	35Tyr	64.15
3k	-9.73	38Lys	31His,35Tyr, 162Trp	59.14
3l	-6.06	NF	31His,35Tyr, 162Trp	13.51
3m	-7.67	35Tyr	31His, 35Tyr	11.54

^aIn this studio were used the diasteremers most stable for each derivates. The energy unit is Kcal/mol. ^bDocking energies on Superoxido Dismustase (SOD), ^cProliferation growth inhibition (PGI) on promastigotes of *L.braziliensis*,

^dFor the compound **3c** no poses were found in active site of SOD enzyme of *T.cruzi* parasite. N.F.: not found.

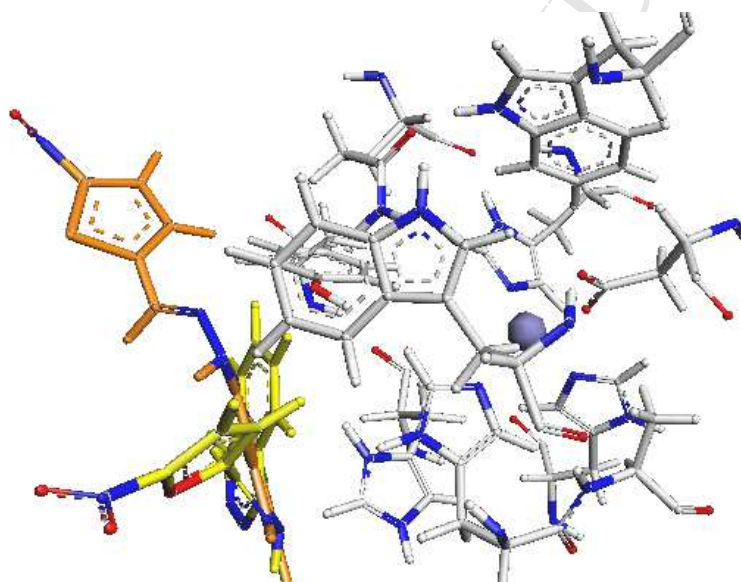


Figure 7. Localization of iron metal and phthalazines **3l** (yellow colour) and **3m** (orange colour) into binding site of SOD.

Finally, in order to discard another inhibitory action of our promising compound **3l**, its inhibitory effect on an important *Leishmania* enzyme such as the dihydrofolate reductase (DHFR) was explored. This enzyme is crucial in the thymine pathway formation that has an important role in the biosynthesis of ADN of the parasite [25e]. Susceptibility to our compound and miltefosine, as well as the antifolate drugs methotrexate as positive control,

was assessed in the absence and presence of folinic acid at different concentration 5 nM, 50 nM and 500 nM as described in literature [43], and the data obtained was shown in Figure 8. Folinic acid is an important substrate of the DHFR enzyme. From Figure 8, it should be noted that the presence of folinic acid clearly does not have effect on the promastigote growth when the parasite are treated with the compound **31** and the reference drug miltefosine, while the parasites treated with the antifolate methotrexate drug showed a significant increase at increasing concentration of folinic acid. Thus, these evidences permit us to discard completely to the dihydrofolate reductase inhibition as possible mode of action of the phthalazine **31** on the antileishmanicidal activity.

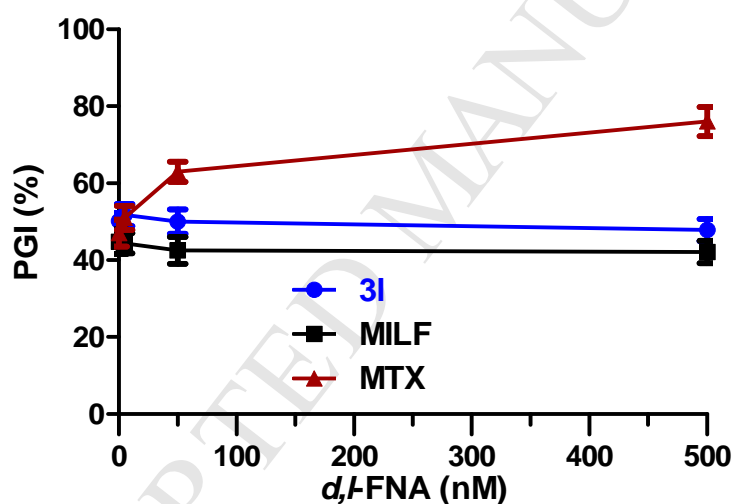


Figure 8. *In vitro* inhibitory effect of **31**, methotrexate (MTX) and miltefosine (MILT) for promastigote of *L.braziliensis* in the absence or presence of *d,l*-folinic acid (FNA). Results are presented as the PGI (%) in the absence or presence of increasing concentration of *d,l*-FNA. Results correspond to averages of three independent experiments with less than 10% SD.

In summary, our preliminary *in vitro* mechanistic assays and *in silico* studies permit us to suggest that the therapeutic effect of **31** may be mainly associated to the induction of oxidative stress generated by potential bio-reduction of nitro group of **31** and the production

of nitric oxide induced in infected macrophage cells. However, additional more specific assays related to oxidative stress induced by the compound **3l** are required for future investigations in order to know the real nature of this possible mechanism of action. Other possible mechanism of action such as inhibition of the enzymes SOD and DHFR were discarded for the most active derivative **3l**.

As last topic, employing the software ChemBioDraw Ultra suite [44a], the selected phthalazines **3a-t** were subjected to the Lipinski's rule of five analysis (drug-likeness) [44b], which helps to predict and explain biological behaviour of small molecules such as phthalazine compound synthesized. The result showed that the active derivative followed the Lipinski rule, with a molecular weight <500 g/mol, a log *P* <5 around 2,94 and 3,47 for **3l** and **3m**, respectively, and these have only 6 or 7 possible interaction of hydrogen (see Table 8). In particular, the most active derivatives **3l** and **3m** exhibited the lowest Log *P*, by which these compounds should present a better passive diffusion than the rest of derivatives into cells, explaining their significant biological response. Therefore, this hypothesis permits to explain the significant anti-leishmanicidal activity of the compounds **3l** and **3m** in comparison with **3c**. Finally, the synthesized phthalazines present theoretically a minor solubility at acidic pH due to the generation of protonated species, which could help to its absorption in the upper digestive tract for *in vivo* assays.

Table 6. Calculated theoretical parameters of the Lipinski's ruler.

Entry	Product	Molecular Weight	Log <i>P</i> pH 7.4	Log <i>P</i> pH 3.0	n-OHNH donors	n-ON Acceptors	Lipinski's Violations
1	3a	282.73	4.36	3.73	1	4	0
2	3b	300.72	4.52	3.86	1	5	0
3	3c	327.73	3.89	3.69	1	6	0
4	3d	361.62	5.19	4.62	1	4	0
5	3e	316.03	4.92	4.35	1	4	0
6	3f	327.73	3.89	3.69	1	6	0

7	3g	361.62	5.19	4.62	1	4	0
8	3h	316.03	4.92	4.35	1	4	0
9	3i	298.73	3.97	3.34	2	5	0
10	3j	357.06	3.82	3.62	1	7	0
11	3k	272.05	2.98	2.41	1	5	0
12	3l	317.03	1.64	1.64	1	7	0
13	3m	333.01	2.20	2.20	1	6	0
14	3n	312.75	3.54	3.30	2	5	0
15	3o	341.75	3.65	3.65	1	6	0
16	3p	375.65	4.75	4.58	1	4	0
17	3q	341.75	3.65	3.65	1	6	0
18	3r	296.75	3.92	3.69	1	4	0
19	3s	364.01	5.04	4.93	1	4	0
20	3t	364.01	5.04	4.93	1	4	0

3. Conclusion

New monoarylhydrazinyl-phthalazines **3a-t** were synthesized through two step of reaction and tested as antileishmanial agents against *L. braziliensis*. Among the tested compounds, the derivatives **3l** and **3m** have shown a significant *in vitro* activity against promastigotes of *L.braziliensis* strain at nano and sub-micromolar levels of EC₅₀, inclusive superior to the drug standard Miltefosine. In particular, the derivative **3l** demonstrated to have low toxicity on macrophage cells with a good selectivity index of 117. This derivative **3l** also exhibited a specific anti-leishmanicidal activity against clinically relevant intracellular amastigotes of *L.braziliensis*, without affecting the viability of the host cells. A structure-activity relationship analysis suggests that a highly conjugated hydrazinyl-nitroheteroaryl group represents an interesting pharmacophore, being the main responsible of the biological activity observed for the investigated phthalazines **3a-t**. The significant antileishmanicidal activity found for the derivative **3l** can be explained by an oxidative stress mechanism induced by metabolized compound **3l** into the pathogen. Finally, the results demonstrate that

the compound **31** represents a promising candidate against *L.braziliensis* and additional assays related to toxicity on human cell lines such as HEPG2, genotoxicity assays and *in vivo* experiments are required to estimate its real potential.

4. Experimental

4.1. Chemistry

Melting points are recorded with a micro melting point apparatus und uncorrected. ^1H NMR, ^{13}C NMR and NOESY spectra are recorded at JEOL Eclipse Plus 400 and JEOL Eclipse Plus 270. Proton chemical shifts were given in relative to tetramethylsilane (δ 0.00 ppm) in $\text{DMSO-}d_6$. Multiplicity is indicated as follows: s (singlet), d (doublet), t (triple), m (multiplet), dd (doublet of doublets), br s (broad singlet), and coupling constant are given in Hz. Carbon chemical shifts are internally referenced to the deuterated solvent signals in CDCl_3 (δ 77.00 ppm). Absorption maxima (λ_{max}) was measured in methanol as solvent on a Varian Cary 1E spectrophotometer (Accuracy: \pm 2 nm). IR spectra were recorded on NICOLET Magna IR 760 using KBr tablets. Elemental analyses of the synthesized compounds were performed using a Perkin Elmer 2400 CHN analyser: results fell in the range of 0.4% of the required theoretical values. Reagents were obtained from Aldrich or Merck companies, and used without previous purification.

4.1.1.- Procedure for the synthesis of 1-chloro-4-hydrazinphthalazine (2): This compound was prepared by a modified procedure previously reported in literature [31a-c]. 1,4-dichlorophthalazine **1** (2.01 g; 10 mmol) was added to a hot solution of hydrazine hydrate (4 mL, 84 mmol) in 20 mL of ethanol, and the mixture was stirred and heated under reflux for 45 minutes. The reaction was cooled at room temperature and the resulting solid was

collected by filtration, washed with cold water (3x20 mL) and dried under vacuum to give a white solid (1.63 g; 83%).

1-chloro-4-hydrazin-phthalazine 2. White solid, 1.63 g (yield 83%); m.p. 200 °C (decomp.) (Lit. 200°C decomp.) [31a,c]. FT-IR (v, cm^{-1}): 3250 (st. N-H), 3164 (st. N-H), 1642 (st. C=N), 1580-1564-1519 (st. C=C). ^1H NMR (400 MHz, $\text{DMSO-}d_6$): δ 8.29 (d, 1H, $J=7.7$ Hz); 8.10-7.90 (m, 3H), 7.35 (s, 3H, NH-NH₂). ^{13}C NMR (100 MHz, $\text{DMSO-}d_6$): δ 133.2 (2C); 132.8; 125.3; 125.1 (2C); 123.1 (2C). Anal. Calcd for $\text{C}_8\text{H}_7\text{ClN}_4$: C, 49.37; H, 3.63; N, 28.79. Found: C, 49.17; H, 3.56; N, 28.50.

4.1.2.- General procedure for the synthesis of 1-(2-benzylidenehydrazyl)-4-chlorophthalazines 3a-m

These derivatives were prepared following a similar procedure reported in literature [31c]. The corresponding aryl or heteroarylaldehyde (0.6 mmol) was added drop wise to a solution of **2** (100 mg, 0.5 mmol) in HCl (5 mL, 1M). The mixture was stirred and heated at 60 °C for 15 minutes, cooled at room temperature and neutralized with sodium hydroxide solution (10%) until to pH 7. The resulting solid was filtered, washed with cold water (3x15 mL) and dried under vacuum to give yellow or orange solids. In general, products were purified by recrystallization from ethanol or mixture ethanol/DMF depending of product **3a-m**, obtaining in the most case prepared the pure diastereoisomer (*E* or *Z*) according to their respective ^1H -NMR spectra. In a few cases (**3c**, **3d**, **3e**, **3f**, **3l** and **3m**), it was obtained a diastereoisomeric mixture and further purifications by recrystallization and chromatography using different solvent mixture did not permit to separate the two diastereoisomers. These cases were reported as a mixture (*E/Z*) and the proportion of the isomers was determined taking into account the differences of intensity between the ylidene proton signal around 8.47-8.58 ppm

corresponding to the *E*-isomer and the signal appeared to 8.75-8.85 of the *Z*-isomer in ¹H-NMR spectra.

4.1.2.1.- 1-(2-benzylidenehydrazyl)-4-chlorophthalazine 3a. Recrystallization solvent ethanol. Yellow solid, 141 mg (yield 96%), 100% *E*-diastereoisomer, m.p. 173-174 °C (Lit. 175-176°C) [31c]. FT-IR (ν , cm⁻¹): 3391 (st. N-H), 2920-2890 (st. C-H), 1618 (st. C=N), 1578-1562-1537 (st. C=C). ¹H NMR (400 MHz, DMSO-*d*₆): δ 12.21 (s, 1H, N-H); 8.47 (s, 1H, N=C-H); 8.37 (d, 1H, *J*=5.8 Hz); 8.00 (d, 2H, *J*=4.8 Hz); 7.88 (m, 3H); 7.43 (m, 3H). ¹³C NMR (100 MHz, DMSO-*d*₆): δ 150.3; 143.7; 136.1; 132.6; 131.2; 129.2; 129.5 (2C); 128.2 (2C); 128.0; 126.1; 123.9; 123.5; 122.4. DEPT-135 (100 MHz, DMSO-*d*₆): δ 136.0; 132.6; 131.2; 129.5 (2C); 128.2 (2C); 128.0; 123.5; 122.4. Anal. Calcd for C₁₅H₁₁ClN₄: C, 63.72; H, 3.92; N, 19.82. Found: C, 63.66; H, 3.85; N, 19.73.

4.1.2.2.- 1-(2-(4-fluorobenzylidene)hydrazyl)-4-chlorophthalazine 3b. Recrystallization solvent ethanol. Yellow solid, 131 mg (yield 92%), 100% *E*-diastereoisomer, m.p. 184-186 °C. FT-IR (ν , cm⁻¹): 3392 (st. N-H), 2920-2890 (st. C-H), 1619 (st. C=N), 1585-1525 (st. C=C). ¹H NMR (400 MHz, *J* Hz, DMSO-*d*₆): δ 12.22 (s, 1H, N-H); 8.46 (s, 1H, N=C-H); 8.36 (d, 1H, *J*=8.0 Hz); 8.07 (dd, 2H, *J*₁=8.8 Hz; *J*₂=8.8 Hz); 7.87 (m, 3H); 7.27 (dd, 2H, *J*₁=8.8 Hz; *J*₂=9.2 Hz). ¹³C NMR (100 MHz, *J* Hz, DMSO-*d*₆): δ 165.1; 162.6; 150.3; 147.6; 143.6; 136.1; 132.5; 130.6 (*J*_{C-C-F}=8.1 Hz) (2C); 128.0; 123.5; 123.2 (*J*_{C-F}=170.2 Hz); 122.7; 116.6 (*J*_{C-F}=22.83) (2C). DEPT-135 (100 MHz, DMSO-*d*₆): δ 136.1; 132.5; 130.6 (2C); 128.0; 123.5; 123.2; 116.6 (2C). ¹⁹F NMR (70 MHz, DMSO-*d*₆): δ -109.35. Anal. Calcd for C₁₅H₁₀ClFN₄: C, 59.91; H, 3.35; N, 18.63. Found: C, 59.84; H, 3.30; N, 18.57.

4.1.2.3.- 1-(2-(4-nitrobenzylidene)hydrazyl)-4-chlorophthalazine 3c. Recrystallization solvent: ethanol/DMF (8/2). Orange solid, 154 mg (yield 94%), isomer mixture (*E/Z*) (94/6), m.p. 255-257 °C. FT-IR (ν , cm⁻¹): 3400 (st. N-H), 2920-2890 (st. C-H), 1626 (st. C=N),

1600-1564-1516 (st. C=C). ^1H NMR (400 MHz, DMSO- d_6): δ 12.58 (s, 1H, N-H); 8.58 (s, 1H, N=C-H); 8.40 (d, 1H, $J=7.7$ Hz); 8.32-8.26 (d, 4H, $J=9.5$ Hz); 7.95-7.87 (m, 3H). ^{13}C NMR (100 MHz, DMSO- d_6): δ 152.5; 149.8; 148.2; 142.3; 138.6; 134.1; 133.8; 129.4 (2C); 127.8; 126.5; 125.7; 125.3; 124.3 (2C). Anal. Calcd for $\text{C}_{15}\text{H}_{10}\text{ClFN}_5\text{O}_2$: C, 54.97; H, 3.08; N, 21.37. Found: C, 54.85; H, 2.98; N, 21.28.

4.1.2.4.- 1-(2-(4-bromobenzylidene)hydrazyl)-4-chlorophthalazine 3d. Recrystallization solvent: ethanol/DMF (9/1). Yellow solid, 121 mg (yield 91%), isomer mixture (*E/Z*) (96/4), m.p. 220-222 °C. FT-IR (ν , cm^{-1}): 3410 (st. N-H), 2920-2890 (st. C-H), 1627 (st. C=N), 1600-1564-1516 (st. C=C). ^1H NMR (400 MHz, DMSO- d_6): δ 12.33 (s, 1H, N-H); 8.44 (s, 1H, N=C-H); 8.36 (d, 1H, $J=7.3$ Hz); 7.99 (d, 2H, $J=8.1$ Hz); 7.87 (m, 3H); 7.64 (d, 2H, $J=7.7$ Hz). ^{13}C NMR (100 MHz, DMSO- d_6): δ 153.7; 148.8; 137.8; 135.1; 133.7; 133.6; 132.0 (2C); 130.6 (2C); 128.0; 126.4; 125.6; 125.1; 123.8. Anal. Calcd for $\text{C}_{15}\text{H}_{10}\text{BrClN}_4$: C, 49.82; H, 2.79; N, 15.49. Found: C, 49.74; H, 2.68; N, 15.38.

4.1.2.5.- 1-(2-(4-chlorobenzylidene)hydrazyl)-4-chlorophthalazine 3e. Recrystallization solvent: ethanol/DMF (9/1). Yellow solid, 108 mg (yield 88%), isomer mixture (*E/Z*) (93/7), m.p. 203-205°C. FT-IR (ν , cm^{-1}): 3412 (st. N-H), 2920-2890 (st. C-H), 1626 (st. C=N), 1600-1564-1516 (st. C=C). ^1H NMR (400 MHz, DMSO- d_6): δ 12.33 (s, 1H, N-H); 8.47 (s, 1H, N=C-H); 8.36 (d, 1H, $J=7.9$ Hz); 8.06 (d, 2H, $J=8.4$ Hz); 7.87 (m, 3H); 7.50 (d, 2H, $J=8.4$ Hz). ^{13}C NMR (100 MHz, DMSO- d_6): δ 153.6; 148.8; 135.0; 134.8; 133.65; 133.62; 130.4 (2C); 129.7; 129.2 (2C); 128.0; 125.7; 125.1; 126.4. Anal. Calcd for $\text{C}_{15}\text{H}_{10}\text{Cl}_2\text{N}_4$: C, 56.80; H, 3.18; N, 17.66. Found: C, 56.74; H, 3.11; N, 17.58.

4.1.2.6.- 1-(2-(3-nitrobenzylidene)hydrazyl)-4-chlorophthalazine 3f. Recrystallization solvent: ethanol/DMF (8/2). Yellow solid, 147 mg (yield 90%), 100% *E*-diastereoisomer, m.p. 235-238 °C. FT-IR (ν , cm^{-1}): 3390 (st. N-H); 3052 (st. N-H), 2920-2890 (st. C-H), 1620

(st. C=N), 1602-1565-1510 (st. C=C). ^1H NMR (400 MHz, DMSO- d_6): δ 12.22 (s, 1H, N-H); 8.88 (s, 1H); 8.59 (s, 1H, N=C-H); 8.42 (d, 1H, $J=7.3$ Hz); 8.38 (d, 1H, $J=7.3$ Hz); 8.21 (d, 1H, $J=8.1$ Hz); 7.87 (m, 3H); 7.72 (dd, 1H, $J_1=8.1$ Hz; $J_2=8.1$ Hz). ^{13}C NMR (100 MHz, DMSO- d_6): δ 152.6; 149.4; 149.0; 137.8; 135.0; 134.1; 133.9; 133.7; 130.6; 127.8; 126.5; 125.7; 125.2; 124.6; 122.6. DEPT-135 (100 MHz, DMSO- d_6): δ 135.0; 134.1; 133.9; 133.7; 130.6; 125.7; 125.2; 124.6; 122.6. Anal. Calcd for $\text{C}_{15}\text{H}_{10}\text{ClFN}_5\text{O}_2$: C, 54.97; H, 3.08; N, 21.37. Found: C, 54.87; H, 3.03; N, 21.32.

4.1.2.7.- 1-(2-(3-bromobenzylidene)hydrazyl)-4-chlorophthalazine 3g. Recrystallization solvent: ethanol/DMF (9/1). Yellow solid, 121 mg (87%), 100% *E*-diastereoisomer, m.p. 217-218 °C. FT-IR (ν , cm^{-1}): 3448 (st. N-H); 3050 (st. C-H), 2920-2890 (st. C-H), 1655 (st. C=N), 1613-1563-1520 (st. C=C). ^1H NMR (400 MHz, DMSO- d_6): δ 12.43 (s, 1H, N-H); 8.45 (s, 1H, N=C-H); 8.37 (d, 1H, $J=7.3$ Hz); 7.92-7.84 (m, 4H); 7.58 (d, 1H, $J=7.7$ Hz); 7.39 (dd, 2H, $J_1=8.1$ Hz; $J_2=8.1$ Hz). ^{13}C NMR (100 MHz, DMSO- d_6): δ 153.3; 149.1; 138.3; 138.0; 133.8; 133.7; 132.9; 131.2; 130.3; 128.3; 127.9; 126.4; 125.7; 125.1; 122.8. Anal. Calcd for $\text{C}_{15}\text{H}_{10}\text{BrClN}_4$: C, 49.82; H, 2.79; N, 15.49. Found: C, 49.76; H, 2.73; N, 15.44.

4.1.2.8.- 1-(2-(3-chlorobenzylidene)hydrazyl)-4-chlorophthalazine 3h. Recrystallization solvent: ethanol/DMF (9/1). Yellow solid, 105 mg (yield 88%), 100% *E*-diastereoisomer, m.p. 196-198 °C. FT-IR (ν , cm^{-1}): 3448 (st. N-H); 3052 (st. C-H), 2920-2890 (st. C-H), 1655 (st. C=N), 1614-1600-1564-1521 (st. C=C). ^1H NMR (400 MHz, DMSO- d_6): δ 12.43 (s, 1H, N-H); 8.46 (s, 1H, N=C-H); 8.37 (d, 1H, $J=8.1$ Hz); 8.32 (s, 1H); 7.89-7.86 (m, 4H); 7.49-7.45 (m, 2H). ^{13}C -NMR (100 MHz, DMSO- d_6): δ 153.4; 149.2; 138.1; 138.0; 134.2; 133.9; 133.7; 130.9; 130.1; 127.9, 127.8; 127.4; 126.4; 125.7; 125.1. DEPT-135 (100 MHz, DMSO-

d_6): δ 153.4; 133.9; 133.7; 130.9; 130.1; 127.9; 127.4; 125.7; 125.1. Anal. Calcd for $C_{15}H_{10}Cl_2N_4$: C, 56.80; H, 3.18; N, 17.66. Found: C, 56.71; H, 3.11; N, 17.56.

4.1.2.9.- 1-(2-(2-hydroxybenzylidene)hydrazyl)-4-chlorophthalazine 3i. Recrystallization solvent: ethanol. Yellow solid, 101 mg (yield 87%), 100% *Z*-diastereoisomer, m.p. 158-160 °C (Lit. 162-163) [31c]. FT-IR (ν , cm^{-1}): 3472 (st. N-H); 3235 (st. O-H); 3052 (st. N-H), 2920-2890 (st. C-H), 1625 (st. C=N), 1600-1580-1532 (st. C=C). 1H NMR (400 MHz, DMSO- d_6): δ 10.45 (s, 1H, N-H); 9.20 (s, 1H, N=C-H); 9.00 (s, 1H, OH); 8.30-8.10 (m, 5H); 7.35 (dd, 1H, $J_1=7.0$ Hz; $J_2=7.0$ Hz); 6.99 (d, 1H, $J=8.4$ Hz); 6.93 (dd, 1H, $J_1=7.3$ Hz; $J_2=7.7$ Hz). ^{13}C NMR (100 MHz, DMSO- d_6): δ 163.4; 159.2; 157.7; 133.8; 133.6; 131.9; 131.4; 130.5; 126.3; 125.6; 120.2; 119.9, 118.7; 117.1; 116.7. DEPT-135 (100 MHz, DMSO- d_6): δ 163.4; 133.8; 133.6; 131.4; 125.6; 120.2; 119.9; 117.1; 116.7. Anal. Calcd for $C_{15}H_{11}ClN_4O$: C, 60.31; H, 3.71; N, 18.76. Found: C, 60.25; H, 3.63; N, 18.66.

4.1.2.10.- 1-(2-(2-methoxy-4-nitrobenzylidene)hydrazyl)-4-chlorophthalazine 3j. Recrystallization solvent: ethanol. Yellow solid, 122 mg (yield 91 %), 100% *E*-diastereoisomer, m.p. 246-248 °C. FT-IR (ν , cm^{-1}): 3330 (st. N-H); 3052 (st. N-H), 2920-2890 (st. C-H), 1621 (st. C=N), 1581-1564-1514 (st. C=C). 1H NMR (400 MHz, DMSO- d_6): δ 12.65 (br, 1H, N-H); 9.24 (d, 1H, $J=2.6$ Hz); 8.69 (s, 1H, N=C-H); 8.39 (d, 1H, $J=7.3$ Hz); 8.27 (dd, 1H, $J_1=9.0$ Hz; $J_2=2.6$ Hz); 7.87 (m, 4H), 4.02 (s, 3H, OCH₃). ^{13}C -NMR (100 MHz, DMSO- d_6): δ 163.22; 163.18; 162.9; 149.6; 141.9; 133.8; 127.3; 126.5; 126.1; 125.8; 125.2; 123.0; 117.9; 112.9; 112.8; 57.5 (O-CH₃). Anal. Calcd for $C_{16}H_{12}ClN_5O_3$: C, 53.72; H, 3.38; N, 19.58. Found: C, 53.65; H, 3.35; N, 19.50.

4.1.2.11.- 1-(2-(furan-2-ylmethylene)hydrazyl)-4-chlorophthalazine 3k. Recrystallization solvent: ethanol. Yellow solid, 122 mg (yield 89 %), 100% *E*-diastereoisomer, m.p. 170-172 °C. FT-IR (ν , cm^{-1}): 3390 (st. N-H), 3075 (st. C-H); 2920-2890 (st. C-H), 1630 (st. C=N),

1573-1537 (st. C=C). ^1H NMR (400 MHz, DMSO- d_6): δ 12.00 (s, 1H, N-H); 8.33 (d, 1H, $J=7.7$ Hz); 8.31 (s, 1H, N=C-H); 7.83 (m, 4H); 7.11 (d, 1H, $J=3.3$ Hz); 6.66 (dd, 1H, $J_1=3.3$ Hz; $J_2=1.8$ Hz). ^{13}C NMR (100 MHz, DMSO- d_6): δ 151.0; 148.5; 145.7; 143.9; 133.9; 133.7; 128.1; 127.2; 126.3; 125.7; 125.0; 114.2; 113.0. Anal. Calcd for $\text{C}_{13}\text{H}_9\text{ClN}_4\text{O}$: C, 57.26; H, 3.33; N, 20.55. Found: C, 57.21; H, 3.30; N, 20.49.

4.1.2.12.- 1-(2-(5-nitrofuranyl)methylene)hydrazyl)-4-chlorophthalazine 3l.

Recrystallization solvent: ethanol/DMF (8/2). Orange solid, 149 mg (yield 93 %), isomer mixture (*E/Z*) (93/7), m.p. 230-232 °C. FT-IR (ν , cm^{-1}): 3353 (st. N-H); 3052 (st. C-H), 2920-2890 (st. C-H), 1612 (st. C=N), 1565-1510 (st. C=C). ^1H NMR (400 MHz, DMSO- d_6): δ 12.57 (s, 1H, N-H); 8.40 (d, 1H, $J=8.1$ Hz); 8.34 (s, 1H, N=C-H); 7.93 (m, 3H); 7.83 (d, 1H, $J=4.0$ Hz); 7.53 (d, 1H, $J=3.8$ Hz). ^{13}C NMR (100 MHz, DMSO- d_6): δ 154.5; 152.2; 141.4; 137.1; 134.4; 133.9; 126.6; 125.9; 125.8; 125.5; 120.0; 115.9; 114.4. DEPT-135 (100 MHz, DMSO- d_6): δ 134.4; 133.9; 125.8; 125.5; 120.0; 115.9; 114.4. Anal. Calcd for $\text{C}_{13}\text{H}_8\text{ClN}_5\text{O}_3$: C, 49.15; H, 2.54; N, 22.04. Found: C, 49.12; H, 2.50; N, 21.98.

4.1.2.13.- 1-(2-(5-nitrothiophen-2-ylmethylene)hydrazyl)-4-chlorophthalazine 3m.

Recrystallization solvent: ethanol/DMF (8/2). Orange solid, 111 mg (yield 85%), isomer mixture (*E/Z*) (94/6), m.p. 220-222 °C. FT-IR (ν , cm^{-1}): 3400 (st. N-H); 3052 (st. N-H), 2920-2890 (st. C-H), 1606-1566-1510 (st. C=C). ^1H NMR (400 MHz, DMSO- d_6): δ 12.59 (s, 1H, N-H); 8.38 (d, 1H, $J=7.7$ Hz); 8.33 (s, 1H, N=C-H); 7.92 (m, 3H); 7.81 (d, 1H, $J=4.0$ Hz); 7.51 (d, 1H, $J=4.0$ Hz). ^{13}C -NMR (100 MHz, DMSO- d_6): δ 154.5; 152.2; 150.3; 141.7; 139.4; 134.4; 133.9; 127.3; 126.6; 125.8; 125.5; 115.9; 114.5. DEPT-135 (100 MHz, DMSO- d_6): δ 141.7; 134.4; 133.9; 125.8; 125.5; 115.9; 114.5. Anal. Calcd for $\text{C}_{13}\text{H}_8\text{ClN}_5\text{O}_2\text{S}$: C, 46.78; H, 2.42; N, 20.98. Found: C, 46.72; H, 2.38; N, 20.93.

4.1.3.- General procedure for the synthesis of 1-(aryl)ethylidene)hydrazyl)-4-chlorophthalazines 3n-t:

To a solution of **2** (100 mg, 0.52 mmol) in HCl (5 mL, 1M) was added the corresponding benzophenone (0.62 mmol). The mixture was stirred and heated at 60 °C for 15 minutes, cooled at room temperature and neutralized with sodium hydroxy until to reach pH 7. The resulting solid was filtered, washed with cold water (3x15 mL) and dried under vacuum to give desired compounds as yellow or orange solids. The product was purified by recrystallization from ethanol, methanol or mixture ethanol/DMF depending of product, obtaining a pure diastereoisomer for all synthesized phthalazines **3n-t** (*E* or *Z*) according to the ¹H-NMR spectra.

4.1.3.1.- 1-(2-(1-(4-hydroxyphenyl)ethylidene)hydrazyl)-4-chlorophthalazine **3n**.

Reaction time: 1 h. Recrystallization solvent: methanol. Yellow solid, 166 mg (yield 97%), 100% *E*-diastereoisomer, m.p. 212-214 °C. FT-IR (ν, cm⁻¹): 3500-3100 (st. O-H); 3318 (st. N-H), 2920-2890 (st. C-H), 1620 (st. C=N), 1598-1574-1513 (st. C=C). ¹H NMR (400 MHz, δ ppm, *J* Hz, DMSO-*d*₆): 12.20 (s, 1H, N-H); 8.40 (d, 1H, *J*=5.5 Hz); 7.96 (d, 2H, *J*=8.4 Hz); 7.82 (m, 3H); 6.79 (d, 2H, *J*=8.8 Hz); 2.45 (s, 3H, CH₃). ¹³C NMR (100 MHz, δ ppm, DMSO-*d*₆): 159.9; 159.3; 146.1; 137.4; 133.5; 133.3; 130.0; 129.2 (2C); 128.5; 126.2; 125.5; 125.0; 115.4 (2C); 14.3 (CH₃). Anal. Calcd for C₁₆H₁₃ClN₄O: C, 61.44; H, 4.19; N, 17.91. Found: C, 61.38; H, 4.15; N, 17.85.

4.1.3.2.- 1-(2-(1-(4-nitrophenyl)ethylidene)hydrazyl)-4-chlorophthalazine **3o**.

Reaction time: 2 h. Recrystallization solvent: ethanol/DMF (8/2) (Orange solid, 138 mg (yield 79%), 100% *E*-diastereoisomer, m.p. 234-236 °C. FT-IR (ν, cm⁻¹): 3392 (st. N-H), 2920-2890 (st. C-H), 1619 (st. C=N), 1585-1525 (st. C=C). ¹H NMR (400 MHz, *J* Hz, DMSO-*d*₆): δ 12.29 (s, 1H, N-H); 8.48 (d, 1H, *J*=6.6 Hz); 8.41 (d, 2H, *J*=8.1 Hz); 8.22 (d, 2H, *J*=8.4 Hz); 7.89

(m, 3H); 2.50 (s, 3H, CH₃). ¹³C NMR (100 MHz, DMSO-*d*₆): δ 157.6; 148.0; 147.9; 145.2; 138.2; 133.8; 133.7; 128.5 (2C); 126.4; 125.6; 125.6; 125.5; 123.7 (2C); 14.3 (CH₃). DEPT-135 (100 MHz, δ ppm, DMSO-*d*₆): 133.8; 133.7; 128.5 (2C); 125.6; 125.5; 123.7(2C) ; 14.3 (CH₃). Anal. Calcd for C₁₆H₁₂ClN₅O₂: C, 56.23; H, 3.54; N, 20.49. Found: C, 56.08; H, 3.41; N, 20.39.

4.1.3.3.- 1-(2-(1-(4-bromophenyl)ethylidene)hydrazyl)-4-chlorophthalazine 3p. Reaction time: 12 h. Recrystallization solvent: ethanol. Yellow solid, 169 mg (yield 88%), 100% *E*-diastereoisomer, m.p. 182-184 °C. FT-IR (ν, cm⁻¹): 3450 (st. N-H), 2940-2890 (st. C-H), 1618 (st. C=N), 1600-1564-1516 (st. C=C). ¹H NMR (400 MHz, *J* Hz, DMSO-*d*₆): δ 12.58 (s, 1H, N-H); 8.40 (d, 1H, *J*=7.7 Hz); 8.32-8.26 (d, 4H, *J*=9.5 Hz); 7.95-7.87 (m, 3H); 2.50 (s, 3H, CH₃). ¹³C-NMR (100 MHz, DMSO-*d*₆): δ 158.5; 147.0; 138.2; 137.5; 133.5; 133.4; 131.5 (2C); 129.5 (2C); 128.7; 126.3; 125.5; 125.2; 123.3; 14.1 (CH₃). DEPT-135 (100 MHz, DMSO-*d*₆): δ 133.5; 133.4; 131.5 (2C); 129.5 (2C); 125.5; 125.2; 14.1 (CH₃). Anal. Calcd for C₁₆H₁₂BrClN₄: C, 51.16; H, 3.22; N, 14.91. Found: C, 51.11; H, 3.17; N, 14.86.

4.1.3.4.- 1-(2-(1-(3-nitrophenyl)ethylidene)hydrazyl)-4-chlorophthalazine 3q. Reaction time: 10 h. Recrystallization solvent: ethanol/DMF (8/2). Yellow solid, 161 mg (yield 93%), 100% *E*-diastereoisomer, m.p. 217-219 °C. FT-IR (ν, cm⁻¹): 3399 (st. N-H); 3052 (st. N-H), 2920-2890 (st. C-H), 1608 (st. C=N); 1574-1525 (st. C=C). ¹H NMR (400 MHz, *J* Hz, DMSO-*d*₆): δ 12.17 (s, 1H, N-H); 8.83 (dd, 1H, *J*₁=2.2 Hz; *J*₂=2.0 Hz); 8.53 (d, 1H, *J*=8.1 Hz); 8.45 (dd, 1H, *J*₁=5.9 Hz; *J*₂=2.6 Hz); 8.20 (dd, 1H, *J*₁=7.9 Hz; *J*₂=2.2 Hz); 7.87 (m, 3H); 7.69 (dd, 1H, *J*₁=7.9 Hz; *J*₂=8.1 Hz); 2.50 (s, 3H, CH₃). ¹³C NMR (100 MHz, DMSO-*d*₆): δ 157.7; 148.8; 147.4; 146.7; 137.9; 133.7 (2C); 130.2; 128.4; 128.0; 126.4; 125.6; 125.4; 124.1; 121.7; 14.4 (CH₃). DEPT-135 (100 MHz, DMSO-*d*₆): δ 133.7 (2C); 130.2; 125.6; 125.3; 124.1; 121.7;

14.4 (CH₃). Anal. Calcd for C₁₆H₁₂ClN₅O₂: C, 56.23; H, 3.54; N, 20.49. Found: C, 56.08; H, 3.39; N, 20.35.

4.1.3.5.- 1-(2-(1-(phenyl)ethylidene)hydrazyl)-4-chlorophthalazine 3r. Reaction time: 10

h. Recrystallization solvent: ethanol. Yellow solid, 105 mg (yield 73%), 100% *E*-diastereoisomer, m.p. 142-144 °C. FT-IR (ν, cm⁻¹): 3401 (st. N-H); 3052 (st. N-H), 2920-2890 (st. C-H), 1611 (st. C=N), 1602-1572-1535 (st. C=C). ¹H NMR (400 MHz, δ ppm, *J* Hz, DMSO-*d*₆): 11.96 (s, 1H, N-H); 8.43 (d, 1H, *J*=5.5 Hz); 8.11 (m, 2H); 7.84 (m, 3H); 7.41 (m, 3H); 2.07 (s, 3H, CH₃). ¹³C-NMR (100 MHz, DMSO-*d*₆): δ 159.7; 146.7; 139.0; 137.4; 133.6; 133.4; 129.8; 128.7 (3C); 127.4 (2C); 126.2; 125.6; 125.2; 14.4 (CH₃). DEPT-135 (100 MHz, DMSO-*d*₆): δ 133.6; 133.4; 129.8; 128.7 (3C); 127.4 (2C); 126.2; 125.5; 125.2; 14.4 (CH₃). Anal. Calcd for C₁₆H₁₃ClN₄: C, 64.76; H, 4.42; N, 18.88. Found: C, 64.66; H, 4.38; N, 18.83.

4.1.3.6.- 1-(2-(1-(2,4-dichlorophenyl)ethylidene)hydrazyl)-4-chlorophthalazine 3s.

Reaction time: 10 h. Recrystallization solvent: ethanol. Yellow solid, 80 mg (yield 42%), 100% *E*-diastereoisomer, m.p. 166-168 °C. FT-IR (ν, cm⁻¹): 3247 (st. N-H); 3052 (st. C-H), 2920-2890 (st. C-H), 1612 (st. C=N), 1602-1570-1519 (st. C=C). ¹H NMR (400 MHz, *J* Hz, DMSO-*d*₆): δ 12.43 (s, 1H, N-H); 8.37 (d, 1H, *J*=7.3 Hz); 7.92-7.84 (m, 4H); 7.58 (d, 1H, *J*=7.7 Hz); 7.39 (dd, 1H, *J*=8.1 Hz; *J*=8.1 Hz); 2.50 (s, 3H, CH₃). ¹³C NMR (100 MHz, DMSO-*d*₆): δ 159.9; 147.0; 139.0; 137.6; 134.2; 133.6; 133.3; 133.0; 129.6; 128.4; 127.8; 126.3; 125.6; 125.3; 123.1; 18.9 (CH₃). DEPT-135 (100 MHz, DMSO-*d*₆): δ 133.6; 133.3; 133.0; 129.6; 127.8; 125.6; 125.2; 123.1; 18.9 (CH₃). Anal. Calcd for C₁₆H₁₁Cl₃N₄: C, 52.56; H, 3.03; N, 15.32. Found: C, 52.47; H, 2.94; N, 15.26.

4.1.3.7.- 1-(2-(1-(2,5-dichlorophenyl)ethylidene)hydrazyl)-4-chlorophthalazine 3t.

Reaction time: 10 h. Recrystallization solvent: ethanol. Yellow solid, 80 mg (yield 42%),

100% *E*-diastereoisomer, m.p. 166-168 °C. FT-IR (ν , cm^{-1}): 3450 (st. N-H), 2940-2890 (st. C-H), 1618 (st. C=N), 1600-1564-1516 (st. C=C). ^1H NMR (400 MHz, J Hz, $\text{DMSO-}d_6$): δ 12.43 (s, 1H, N-H); 8.37 (d, 1H, $J=7.7$ Hz); 8.32 (d, 1H, $J=9.5$ Hz); 7.89-7.86 (m, 3H); 7.49-7.45 (m, 2H); 2.50 (s, 3H, CH_3). ^{13}C NMR (100 MHz, $\text{DMSO-}d_6$): δ 158.5; 147.0; 138.2; 137.5; 133.5; 133.4; 131.5 (2C); 129.5 (2C); 128.7; 126.3; 125.5; 125.2; 123.3; 14.1 (CH_3). DEPT-135 (100 MHz, $\text{DMSO-}d_6$): δ 133.5; 133.4; 131.5 (2C); 129.5 (2C); 125.5; 125.2; 14.1 (CH_3). Anal. Calcd for $\text{C}_{16}\text{H}_{11}\text{Cl}_3\text{N}_4$: C, 52.56; H, 3.03; N, 15.32. Found: C, 52.06; H, 2.89; N, 15.15.

4.2. Biology

4.2.1. General

Promastigotes of *Leishmania (V.) braziliensis* strain MHOM/CO/87/UA301 (provided by Dr. Carlos Muskus. Programa de Estudio y Control de Enfermedades Tropicales PECET, Universidad de Antioquia, Colombia) were isolated from footpad lesions in BalbC mice previously infected. For differentiation and culture maintenance was used medium LIT (tryptose 15 g/L, yeast extract 5 g/L, liver extract 2 g/L, hemin–NaOH 0.02 g/L, glucose 4 g/L, NaCl 9 g/L, KCl 0.4 g/L Na_2HPO_4 , 7.5 g/L, pH 7.4) supplemented with 10% fetal bovine serum and maintained at 29 °C. Macrophages BMDM were obtained from mouse bone marrow and differentiated in a conditioned medium of mouse lung fibroblasts (medium L-929), as described previous methodologies [39, 45].

4.2.2. Anti-leishmanial activity on promastigote proliferation

In order to evaluate the effect of twenty phthalazines on the promastigotes viability of *L.braziliensis* strain, a colorimetric test, as reported by Saint–Pierre–Chazalet [46a], was performed with modifications. Briefly, 2×10^6 parasites/mL were seeded in a 96-well plate,

adding a unique concentration of 20 μM of each compound, and it was incubated for 96 h at 29 $^{\circ}\text{C}$. After the incubation, 1 mg/mL 3-(4,5-dimethylthiazol-2-yl)-2,5-diphenyl tetrazolium bromide (MTT) was added and then it was incubated in darkness for 4 h. After this time, the parasites were lysed with acidic isopropanol and the plate was read at 570 nm in a spectrophotometer Synergy HT (Biotek) with the software KC43.4 Rev. 21. Miltefosine was used as reference drug. Compounds **3l** and **3m** that generated more than 50% inhibition of promastigote proliferation (compared to untreated parasites) were selected for further evaluation. The EC_{50} calculation of selected compounds was performed using growth curves in LIT medium, as previously reported [46b]. Briefly, the cultures were established at 1×10^6 promastigotes/mL, and were added increasing concentration of **3l** and **3m** from 0.1 to 10 μM at 29 $^{\circ}\text{C}$ in separated experiments. Parasite proliferation was monitored daily by direct counting in a Neubauer chamber; three independent experiments were performed for each concentration of the corresponding compounds.

4.2.3. Assay of cytotoxic activity against mammalian cells.

Murine macrophages (BMDM) cell line were grown in L-929 and maintained at 37 $^{\circ}\text{C}$ in 5% CO_2 and 90% humidity. Macrophages were re-suspended in growth medium at a final concentration of 5×10^4 cells/mL, placed in a 96-well culture microplate (100 μL /well), and incubated with the test drugs for 48 h. Cytotoxicity was assessed by using the colorimetric MTT reduction assay and expressed as percentage of MTT reduction relative to control cells. Increasing concentrations of the mentioned compounds from 10 to 100 μM were tested.

4.2.4. Intracellular amastigotes infections

The effect of the compound **3l** on intracellular amastigotes was performed by the protocol previously described [47]. Briefly, a mixture of macrophages BMDM and promastigotes of *L.*

braziliensis, in a proportion 1:10 diluted in DMEM +10% FBS, was prepared. The mixture was placed on glass coverslips and keeping in a moist chamber for 18 h at 37 °C and 5% CO₂. After, the medium was removed, adding new medium with the tested condition and incubated for 96 h in same condition. Then, macrophages were stained with Giemsa and counted. Increasing concentrations of the mentioned compounds from 10 to 100 µM were tested.

4.2.5. Mechanism of Action Studies

4.2.5.1. Evaluation of Mitochondrial Dehydrogenase Activity.

Mitochondrial dehydrogenase activities were measured in 24-well plates as described the literature [41d]. One million of *L.braziliensis* promastigotes in 500 µL medium were seeded in each well and 20 µM of the compound **31** and miltefosine were added. Two wells with untreated parasites were maintained as controls corresponding to the given time of treatment. The cultures were incubated at 28 °C. At the different incubation times, the promastigotes were counted and the colorimetric MTT dye-reduction assay was performed, with the tetrazolium salt being converted into purple formazan by living mitochondria. Fifty µL of a solution containing 5 mg/mL of MTT in PBS were added to each well and plates were incubated for an additional time of 4 h. The reaction was stopped by the addition of 500 µL of acidic isopropanol (0.4 mL HCl 10 N in 100 mL isopropanol). The absorbance was measured at 570 nm. Under our conditions, compounds did not interfere with the reaction mixture. All the assays were performed by triplicate. Percentage of mitochondrial dehydrogenase activities (Pmdh (%)) were determined using untreated parasites-activities as 100 %.

4.2.5.2. Determination of nitrite concentration

Nitrite (NO_2^-) accumulation was determined in supernatants of infected macrophages with *L.braziliensis* amastigote, which were incubated for 48 h in the presence of the compound **31** at increasing concentrations 0.08 μM , 0.80 μM , 8.0 μM as described above. Three wells with untreated amastigote-macrophage and other three wells with untreated macrophage were incubated as controls corresponding to the given time of treatment. The assay was performed by the Griess reaction (detection limit: 1.56 μM) with sodium nitrite as a standard as previously described [42]. In brief, 100 μL of Griess reagent 1% sulphanilamide in 50% of acetic acid was added to 400 μL of each sample. Blank reference and standard curve were determined. After 15 min, 100 μL of a solution of N-[naphthyl]ethylenediamine dihydrochloride (1%) in acetic acid in 50%. The absorbance was measured at 540 nm. Nitrite content was quantified by the extrapolation from sodium nitrite standard curve in each experiment. All the assays were performed by triplicate. The results were expressed as percentages in comparison with untreated infected macrophages.

4.2.5.3. Dihydrofolate reductase inhibition assays

Dihydrofolate reductase inhibition of the compound **31** and miltefosine, as well as the known antifolate drug methotrexate as positive control, was assessed in absence or presence of folinic acid as described the literature [43]. One million of *L.amazonensis* promastigotes in 200 μL medium were seeded in each well using 0.5 μM of the compounds, 2 μM of methotrexate and 10 μM of miltefosine. Increasing concentrations 5 mM, 50 mM and 500 mM were used on the different cultures. These concentrations inhibited from 40 to 60% of the parasite proliferation. Three wells with untreated parasites were maintained as negative controls. The cultures were incubated at 28 °C for 72 hours as described above. After this time, the PGI was determined by direct counting in a Neubauer chamber, three independent

experiments were performed for each concentration of the corresponding compounds. All the assays were performed by triplicate.

4.2.5.4. Superoxide dismutase inhibition assays

Superoxide dismutase inhibition was determined by action of xantine oxidase. The parasites cultured as described above were centrifuged. Four million of *L.braziliensis* promastigote in 500 μ L medium. Three different concentrations were used for the compound **3I**: 0.012 μ M, 0.12 μ M and 1.2 μ M. The pellet was suspended in 2 mL of sodium chloride-Tris-EDTA (STE) buffer (0.25 M sucrose, 25 mM Tris-HCl, 1M EDTA, pH 7.8) and disrupted by three cycles of sonic disintegration, for 40 s each at 60 V. The sonicated homogenate was centrifuged at 1500 g for 1 min at 4 °C, and the pellet was washed three times with ice-cold STE buffer, giving a total supernatant fraction. This fraction was centrifuged (2500 g for 15 min at 4° C), and the supernatant was collected. The protein concentrations were determined using the Bradford method [48a]. The total superoxide activities were determined using the method described by Oberley [48b], which measures the reduction in nitroblue tetrazolium (NBT) by superoxide ions. Into each bucket, an amount of 47 μ L of xantina (0.122 mM), 23 μ L of EDTA (0.122 mM), 23 μ L of NBT (30.6 mM), 14 μ L of Na₂CO₃ (49 mM), 8 μ L of albumina (0.006%) was added, along with 25 μ L of the parasite homogenate and 10 μ L of xantina oxidase (8.4 U). The mixture was incubated by 30 min at 27° C. Three controls named 100% were treated as described above in absence of xantine oxidase. After this time, to the mixture was added 50 μ L of CuCl₂ (0.8 mM), and then the absorbance (A_o) was measured at 595 nm in a spectrophotometer. All the assays were performed by triplicate. Under these conditions, the reduction of NBT is lineal at increasing concentrations of the pure enzyme CuZn-SOD. The data is described as U/mg protein, a unit of SOD is defined as the necessary amount of SOD to inhibit to a 50% of the NBT reduction.

4.2.6. Molecular modelling studies

The optimized structures of all compounds were obtained by using AM1 method [49], available as part of the ArgusLab 4.0 program [49], where the requested convergence on density matrix was 10^{-13} and the maximum gradient component was 0.000084. The structures were optimized as *E*-diastereomer. Docking calculations and analysis were carried out using the X-ray crystallographic structure of the *T.cruzi* SOD (PDB ID code: 2GCP) as the target. The protein is cocrystallized with iron and magnesium metals. Its structure was minimized using the CHARMM on Swiss-PdbViewer v4.0.1 software [50]. Binding site definition was determined by comparison with reported interactions for the respective co-crystallized ligand. The prepared protein was exported to ArgusLab v.4.0.1 program package and save as Agl document. Then, molecular docking for the most stable extended geometry of the 5 tested derivatives were performed using AMBER method on the selected protein implemented in the ArgusLab (v4.0.1) package program under Windows 7.0 environment. The docking experiment on the tested enzyme was carried out between the energy-minimized ligand into the binding site through their respective grid map dimensions and with a grid point spacing of 0,375 Å. Rigid ligand models were used in the docking and subsequent optimization scheme. As a test of docking accuracy and for docking energy comparison, co-crystallized ligands were re-docked into the protein structures. Different orientations of the ligands were searched and ranked based on their energy scores. Reproducibility of the calculated affinity energy and the minimum energy pose were evaluated through 10 replicates for each ligand [51]. Affinity energy is reported as mean of the 10 replicates. The lowest energy (strongest-docking) poses for each ligand in binding site of the protein are summarized in Table 5.

4.3. Data Analysis

The results of each experimental (section 4.2.2, 4.2.3 and 4.2.4) were analyzed by the method described by Huber and Koella [52]. For calculation of IC₅₀, they used the following mathematical formula: $\log(\text{IC}_{50}) = \log(x_1) + [(y_1 - y_{0/2}) / (y_1 - y_2)] [\log(x_2) - \log(x_1)]$.

4.4. Drug-Like Properties Calculations

The ZDO charges on the ylidene carbon were calculated using semi-empirical method AM1 for each investigated molecules (**3a-s**). This charger was calculated over the optimized geometry of the corresponding stereoisomers of all molecules. The mentioned calculations were performed using ArgusLab 4.0 package [49b]. On the other hands, the properties vinculated to five ruler of each phthalazinyl-hydrazone were separately calculated using ChemBio3D® Ultra 11.0 software package [44a] (Cambridge Soft Corporation, Cambridge, MA, USA) starting from the 3D structure.

Acknowledgments

The autor thanks to Decanato de Investigación y Desarrollo (Universidad Simón Bolívar, Caracas-Venezuela); Grants 2012002132 and 2012000784 from Fondo Nacional de Ciencia y Tecnología (FONACIT-Venezuela) to X.S-M, for finacial support, as well as to the Laboratorio de Resonancia Magnética Nuclear (Laboratorio B, Universidad Simón Bolívar, Caracas) for the spectroscopic facilities and Fundación Instituto de Estudios Avanzados (IDEA) for the biological assays.

Supplementary material

Supplementary material related to this article can be found at www.sciencedirect.com.

References

- [1] "Leishmaniasis Fact sheet N°375". World Health Organization. (<http://www.who.int/mediacentre/factsheets/fs375/en/>).
- [2] P. Desjeux, *Clin. Dermatol.* 1996, 14, 417-423.
- [3] M.J. McConville, D. Souza, E. Saunders, V.A. Likic, N. Thomas, *Trends Parasitol.* 23 (2007) 368–375.
- [4] U. Sharma, S. Singh, *J. Vector Borne Dis.* 45 (2008) 255–272.
- [5] S.L. Croft, G.H. Coombs, *Trends Parasitol.*, 2003, 19, 502-508.
- [6] (a) World Health Organization. (<http://www.who.int/leishmaniasis/en/>). (b) Weekly epidemiological record, World Health Organization, 91 (2016) 285-296. (<http://www.who.int/wer>).
- [7] J. Alvar, I.D. Velez, C. Bern, M. Herrero, P. Desjeux, J. Cano, J. Jannin, M. Den Boer, D. Argaw, S. Bhattacharya, M. Ejov, A.N. Elkhouri, J.A. Ruiz-Postigo, J. Serrano, A. Denereaz, B. Arana, S.M. Robledo, K. Mondragon, A. Velez, L. Lopez, L.A. Acosta, *PLoS One* 7 (2012) e35671.
- [8] M. Den Boer, D. Argaw, J. Jannin, *Clin. Microbiol. Infect.* 17 (2011) 1471.
- [9] E.T. Nascimento, M.L.N Moura, J.W. Queiroz, A.W. Barroso, A.F. Araujo, E.F. Rego, M.E. Wilson, R.D Pearson, S.M. Jeronimo, *Trans. R. Soc. Trop. Med. Hyg.* 105 (2011) 298–300.
- [10] T. Herremans, E. Pinelli, M. Casparie, N. Nozari, J. Roelfsema, L. Kortbeek, *Int Health* 2 (2010) 42–46.
- [11] R. Ignatius, C. Loddenkemper, J. Woitzik, T. Schneider, G. Harms, *Vector-Borne Zoonotic Dis.* 11 (2011) 1213–1215.
- [12] (a) H.C. Maltezou, *J. Biomed. Biotechnol.* 2010 (2010) No. 617521. (b) F. Chappuis, S. Sundar, A. Hailu, H. Ghalib, S. Rijal, R.W. Peeling, J. Alvar, M. Boelaert, *Nat. Rev.*

- Microbiol. 5 (2007) S7-S16. (c) S. Patterson, S. Wyllie, Trends Parasitol. 30 (2014) 289-298.
- (d) F. Frezard, P.S. Martin, M.C.M Barbosa, A.M. Pimenta, W.A. Ferreira, J.E. De Melo, J.B. Mangrum, C. Demicheli, J. Inorg. Biochem. 102 (2008) 656-665.
- [13] (a) E. Palumbo, Am. J. Ther. 16 (2009) 178-182. (b) S.L. Croft, M.P. Barrett, Trends Parasitol. 21 (2005) 508-512. (c) J. Mishra, A. Saxena, S. Singh, Curr. Med. Chem. 14 (2007) 1153-1169. (d) D.O. Santos, C.E.R. Coutinho, M.F. Madeira, C.G. Bottino, R.T. Vieira, A.B. Nascimento, S.C. Bourguignon, S. Corte-Real, R.S. Pinho, C.R. Rodriguez, H.C. Castro, Parasitol. Res., 103 (2008) 1-10.
- [14] (a) (a) N. Singh, Indian J. Med. Res. 123 (2006) 411-422. (b) S. Sundar, D.K. More, M.K. Singh, V.P. Singh, S. Sharma, A. Makharia, P.C. Kumar, H.W. Murray, Clin. Infect. Dis. 31 (2000) 1104-1107.
- [15] S. Sundar, J. Chakravarty, Expert. Opin. Pharmacother. 14 (2012) 53-63.
- [16] (a) A. Fournet, A.A. Barrios, V. Munoz, R. Hocquemiller, A. Cave, J. Bruneton, Antimicrob. Agents and Chemoth. (1993) 859-863. (b) W. Devine, J.L. Woodring, U. Swaminathan, E. Amata, G. Patel, J. Erath, N.E. Roncal, P.J. Lee, S.E. Leed, A. Rodriguez, K. Mensa-Wilmot, R.J. Sciotti, M.P. Pollastri, J. Med. Chem. 58 (2015) 5522-5537.
- [17] K.S. Van Horn, X. Zhu, T. Pandharkar, S. Yang, B. Vesely, M. Vanaerschot, J.C. Dujardin, S. Rijal, D.E. Kyle, Z. Wang, K.A. Werbovetz, R. Manetsch, J. Med. Chem. 57 (2014) 5141-5156.
- [18] Y.S. Birhan, A.A. Bekhit, A. Hymete, Org. Med. Che. Lett. 4 (2014) 10.
- [19] J.D. Berman, M. King, N. Edwards, Antimicrob. Agents Chemother. 33 (1989) 1860-1863.
- [20] A.K. Bhattacharjee, D.J. Skanchy, B. Jennings, T.H. Hudson, J.J. Brendle, K.A. Werbovetz, Bioorg. Med. Chem. 10 (2002) 1979-1989.

- [21] V.J. Ram, A. Goel, M. Verma, I.B. Kaul, A. Kapil, *Bioorg. Med. Chem. Lett.* 4 (1994) 2087–2090.
- [22] K.C. Agarwal, V. Sharma, N. Shakya, S. Gupta, *Bioorg. Med. Chem. Lett.* 19 (2009) 5474–5477.
- [23] S. Kumar, N. Shakya, S. Gupta, J. Sarkar, D.P. Sahu, *Bioorg. Med. Chem. Lett.* 19 (2009) 2542–2545.
- [24] M. Sanchez-Moreno, F. Gómez-Contreras, P. Navarro, C. Marín, I. Ramírez-Macías, F. Olmo, A.M. Sanz, L. Campayo, C. Cano, M.J.R. Yunta, *J. Antimicrob. Chemother.* 67 (2012) 387–397.
- [25] (a) A.H. Fairlamb, I.B.R. Blackburn, *Science*, 227 (1985) 1485-1487. (b) T.J. Benson, J.H. Garforth, *Biochem. J.* 286 (1992) 9-11. (c) W.N. Hunter, S. Bailey, J. Habach, *J. Mol. Biol.* 227 (1992) 322-333. (d) C.R. Caffrey, S. Scory, D. Steverding, *Curr. Drug Targets*, 1 (2000) 155-162. (e) I.H. Gilbert, *Biochim. Biophys. Acta*, 1587 (2002) 249-257. (f) M.W. Nowicki, L.B. Tulloch, L. Worrall, I.W. McNae, V. Hannaert, P.A. Michels, *Bioorg. Med. Chem.* 16 (2008) 5050-5061.
- [26] (a) J.F. Alzate, A.A. Arias, D. Moreno-Mateos, *Mol. Biochem. Parasitol.* 152 (2007) 192-202. (b) A. Genetu, E. Gadisa, A. Aseffa, *Exp. Parasitol.* 113 (2006) 221-226. (c) N. Le Trang, S.R. Meshnick, K. Kitchener, J.W. Eaton, A. Cerami, *J. Biol. Chem.* 258 (1983) 125-130. (d) J.F. Bachege, M.V. Navarro, L. Bleicher, R.K. Bortoleto-Bugs, D. Dive, P. Hoffmann, E. Viscogliosis, R.C. Garratt, *Proteins*, 77 (2009) 26-37. (e) I.G. Muñoz, J.F. Moran, M. Becana, *Protein Sci.* 14 (2002) 387-394.
- [27] (a) M. Rodríguez-Ciria, A.M. Sanz, M.J.R. Yunta, *Bioorg. Med. Chem.* 15 (2007) 2081–91. (b) A.M. Sanz, F. Gomez-Contreras, P. Navarro, *J. Med. Chem.* 51 (2008) 1962–1966. (c) M. Sánchez-Moreno, A.M., Sanz, F. Gómez-Contreras, *J. Med. Chem.* 54 (2011) 970–979.

- (d) A.M. Sanz, F. Gomez-Contreras, P. Navarro, C. Marín, F. Olmo, M.J.R. Yunta, A.M. Sanz, M.J. Rosales, C. Cano, L. Campayo, *J. Med. Chem.* 55 (2012) 9900-9913.
- [28] (a) C. Olea-Azar, C. Rigol, L. Opazo, A. Morello, J.D. Maya, Y. Repetto, G. Aguirre, H. Cerecetto, R. Di Maio, M. Gonzalez, W. Porcal, *J. Chil. Chem. Soc.* 48 (2003) 77. (b) C. Olea-Azar, C. Rigol, F. Mendizabal, A. Morello, J.D. Maya, C. Moncada, E. Cabrera, R. Di Maio, M. Gonzalez, H. Cerecetto, *Free Radical Res.* 37 (2003) 993. (c) C. Olea-Azar, A.M. Atria, R. Di Maio, G. Seoane, H. Cerecetto, *Spectrosc. Lett.* 31 (1998) 849.
- [29] (a) S. Patterson, S. Wyllie, *Trends in Parasitol.* 30 (2014) 289. (b) S. Wyllie, S. Patterson, A.H. Fairlamb, *Antimicrob. Agents Chemother.* 57 (2013) 901-906. (c) S.R. Wilkinson, M.C. Taylor, D. Hom, J.M. Kelly, I. Cheeseman, *PNAS*, 105 (2008) 5022-5027.
- [30] (a) Y. Zhao, Z. Lin, C. He, H. Wu, C. Duan, *Inorg. Chem.* 45 (2006) 10013-10015. (b) D. Attanasio, G. Dessy, V. Fares, *Inorg. Chim. Acta* 104 (1985) 99-107.
- [31] (a) X.Y. Sun, L.P. Guan, L. Zhang, C.X. Wei, H.R. Piao, Z.S. Quan, *J. Braz. Chem. Soc.* 20 (2009) 826-831. (b) A.R. Todeschini, A.L.P. Miranda, K.C.M. Silva, S.C. Parrini, E.J. Barreiro, *Eur. J. Med. Chem.* 33 (1998) 189-199. (c) G. Tarzia, E. Ocelli, E. Toja, D. Barone, N. Corsico, L. Gallico, F. Luzzanill, *J. Med. Chem.* 31 (1988) 1115-1123.
- [32] (a) V.A. Kogan, S.I. Levchenkov, L.D. Popov, I.A. Shcherbakov, *Rus. J. Gen. Chem.*, 79, (2009) 2767-2775. (b) A. Trzesowska-Kruszynska, *Cryst Eng Comm.*, 2015, (DOI: 10.1039/c5ce00846h). (c) E.B. Lindgren, J.D. Yoneda, K.Z. Leal, A.F. Nogueira, T.R.A. Vasconcelos, J.L. Wardell, S.M.S.V. Wardell, *J. Mol. Struct.* 1036, (2012) 19. (d) G. Giorgi, F. Pontecelli, L. Savini, L. Chiasserini, C. Pellerano, *J. Chem. Soc. Perkin Trans. 2*, 2000, 2259. (e) B.I. Buzykin, N.N. Bystrykh, A.P. Stolyarov, S.A. Flegontov, V.V. Zverev, Y.P. Kitaev, *Khim. Geterotsikl. Soedin*, No. 3, 1976, 402. (f) B.I. Buzykin, N.N. Bystrykh, A.P. Stolyarov, S.A. Flegontov, V.V. Zverev, Y.P. Kitaev, *Khim. Geterotsikl. Soedin*, No.9, 1977, 1264. (g) H. Cerecetto, R. Di Maio, M. Gonzalez, M. Risso, G. Sagrera, G. Seoane, A.

Denicola, G. Peluffo, C. Quijano, A.O.M Stoppani, M. Paulino, C. Olea-Azar, M. A. Basombrio, *Eur. J. Med. Chem.*, 35 (2000) 343. (h) L.D Popov, S.I. Levchenkov, I.N. Scherbakov, Z.A. Starikova, E.B. Kaimakan, V.V. Lukov, *Rus. J. Gen. Chem.*, 82, 465. (i) C. Stassinopoulou, *Tetrahedron*, 32, 1976, 1147. (j) R.J. Butcher, J.P. Jasinski, H.S. Yathirajan, A.M. Vijesh, B. Narayama, *Acta Crystallogr. Sect. E: Struct. Rep. Online*, 63, 2007, 3674. (k) B. Hollo, J. Magyari, V. Zivkovic-Radovanovic, G. Vuckovic, Z.D. Tomic, I.M. Szilagyi, G. Pokol, K.M. Szecsenyi, *Polyhedron* 80 (2014) 142-150.

[33] S.L. Croft, K. Selfert, M. Duchene, *Mol. Biochem. Parasitol.* 126 (2003) 165.

[34] (a) Urbina, J.A., DoCampo, R., *Trends Parasitol.* 2003, 19, 495. (b) B.S. Hall, S.R. Wilkinson, *Antimicrob. Agents and Chem.* (2011) 115-123. (c) B.S. Hall, C. Bot, S.R. Wilkinson, *J. Biol. Chem.* 286 (2011) 13088–13095.

[35] E.S. Coimbra, M.R. Antinarelli, A.D. Da Silva, M.L.F. Bispo, C.R. Kaiser, M.V.N. De Souza, *Chem. Biol. Drug. Des.* 81 (2013) 658-665.

[36] A. Baliani, G. Jiménez-Bueno, M.L. Stewart, V. Yardley, R. Brun, M.P. Barrett, I.H. Gilbert, *J. Med. Chem.* 48 (2005) 5570.

[37] (a) N.S. Carter, A.H. Fairlamb, *Nature* 361 (1993) 173-176. (b) N.S. Carter, B.J. Berger, A.H. Fairlamb, *J. Biol. Chem.* 270 (1995) 28153-28157. (c) M.P. Barrett, A.H. Fairlamb, *Parasitol. Today* 15 (1999) 136-140. (d) P. Maeser, A. Luescher, R. Kaminsky, *Drug Resistance Updates* 6 (2003) 281-290. (e) S.M. Landfear, B. Ullman, N.S. Carter, M.A. Sanchez, *Eukaryot. Cell.* 3 (2004) 245-254. (f) H.P. De Koning, S.M. Jarvis, *Mol. Pharmacol.* 56 (1999) 1162-1170.

[38] F.M. Marim, T.N. Silveira, D.S. Lima, D.S. Zamboni, *PLoS One* 5 (2010) e15263.

[39] (a) G.F. Whitmore, A.J. Varghese, *Biochem. Pharmacol.* 35 (1986) 97-103. (b) L.M. De Oliveira et. al. (2010) In *Current Research, Tecnology and Education, Topics in Applied Microbiology and Microbial Biotechnology (Vol. 2)* (Mendez-Vilas, A., ed.), pp 1078-1086.

- [40] R.C. Zauli-Nascimento, D.C. Miguel, J.K.U. Yokoyama-Yasunaka, L.I.A. Pereira, P.A.M. Oliveira, F. Ribeiro-Dias, M.L. Dorta, S.R.B. Uliana, *Trop. Med. Int. Health* 15 (2010) 68.
- [41] (a) L. Boiani, G. Aguirre, M. González, H. Cerecetto, A. Chidichimo, J.J. Cazzulo, M. Bertinaria, S. Guglielmo, S., *Bioorg. Med. Chem.* 16 (2008) 7900-7907. (b) M. Boiani, L. Piacenza, P. Hernández, L. Boiani, H. Cerecetto, M. González, A. Denicola, *Biochem. Pharmacol.* 79 (2010) 1736-1745. (c) M. Maarouf, Y. De Kouchkovsky, S. Brown, P.X. Petit, M. Robert-Gero, *Exp. Cell Res.* 232 (1997) 339-348. (d) A.M. Voets, M. Huigsloot, P.J. Lindsey, A.M. Leenders, W.J. Koopman, P.H. Willems, R.J. Rodenburg, J.A. Smeitink, H.J. Smeets, *Biochim. Biophys. Acta.* 1822 (2012) 1161-1168. (e) B. Van Houten, V. Woshner, J.H. Santos, *DNA Repair (Amst).* 5 (2006) 145-152. (f) M.R. Castro, E. Suarez, E. Kraiselburd, A. Isidro, J. Paz, L. Ferder, S. Ayala-Torres, *Exp Gerontol.* 47 (2012) 29-37. (g) M.F. Alexeyev, *FEBS J.* 276 (2009) 5768-5787. (h) D. Benítez, M. Cabrera, P. Hernández, L. Boiani, M.L. Lavaggi, R. Di Maio, G. Yaluff, E. Serna, S. Torres, M.E. Ferreira, N. Vera de Bilbao, E. Torres, S. Pérez-Silanes, B. Solano, E. Moreno, I. Aldana, A. López de Cerain, H. Cerecetto, M. González, A. Monge, *J. Med. Chem.* 54 (2011) 3624-3636.
- [42] (a) A.C. Andrezza, L. Shao, J.F. Wang, L.T. Young, *Arch Gen Psychiatry.* 67 (2010) 360-368. (b) T.G. Evans, L. Thai, D.L. Granger, J.B. Hibbs Jrs., *J. Immunol.* 151 (1993) 907-915. (c) A.H. Ding, C.F. Nathan, D.J. Stuehr, , *J. Immunol.* 141 (1988) 2407-2412.
- [43] (a) A. Fadilli, D. Richards, C. Kindig, M. Ouellette, *Biochem. Pharmacol.* 66 (2003) 999-1008. (b) E. Osorio, C. Aguilera, N. Naranjo, M. Marin, C. Muskus, *Biomedica*, 33 (2013) 393-401.
- [44] (a) [http://www.cambridgesoft.com/Ensemble_for_Chemistry/ChemBioDraw/ChemBio\(DrawUltra14Suite\)](http://www.cambridgesoft.com/Ensemble_for_Chemistry/ChemBioDraw/ChemBio(DrawUltra14Suite)). (b) C.A. Lipinski, F. Lombardo, B.W. Dominy, P.J. Feeney, *Adv Adv. Drug Deliv. Rev.* 46 (2001) 3-26.

- [45] M.D. Englen, Y.E. Valdez, N.M. Lehnert, B.E. Lehnert, B. E. J. Immunol. Methods 184 (1995) 281.
- [46] (a) M. Saint-Pierre-Chazalet, M. Ben Brahim, L. Le Moyec, C. Bories, M. Rakotomanga, P.M. Loiseau, J. Antimicrob. Chemother. 64 (2009) 993. (b) X. Serrano-Martín, Y. García-Marchan, A. Fernandez, N. Rodriguez, H. Rojas, G. Visbal, G. Benaim, Antimicrob. Agents Chemother. 53 (2009) 1403.
- [47] J. Nuñez-Durán, D. Bompert, J. Charris, J. Camacho, D. Rodríguez, T. Rodríguez, G. Visbal, A. Álvarez, Y. García-Marchan, X. Serrano-Martín, R. F. F. 75 (2012) 50.
- [48] (a) M.M. Bradford, Anal. Biochem. 72 (1976) 248-252. (b) L. Oberley, D. Splitz, Meth. Enzymol. 105 (1984) 457.
- [49] (a) M.J.S. Dewar, E.G. Zoebisch, E.F. Healy, J.J.P. Stewart, AM1: A New General Purpose Quantum Mechanical Model, J. Am. Chem. Soc. 107 (1985) 3902-3909. (b) Thompson, M.A., 2004 , ArgusLab 4.0 Planaria Software LLC, Seattle, WA.
- [50] Guex, N., Peitsch, M., Schwede, T., Diemand, A., DeepView/Swiss-PdbViewer V4.0.1.
- [51] Young, D.C. 2009. Computational Drug Design. A guide for computational and Medicinal Chemistry. USA. John Wiley&Sons inc. P 141.

Highlights

- New phthalazine analogues were designed, synthesized and evaluated against *L.braziliensis*.
- The presence of a highly conjugated nitroheterocyclic moiety plays an important role in the antileishmanial activity of these phthalazines.
- The compound **3l** exhibited a significant response towards promastigote and amastigote stages of parasite, without affecting viability of the macrophage cells.
- The SOD and DHFR inhibition assays and oxidative stress experiments were also conducted.